Bioorganic Chemistry 87 (2019) 534–549

Contents lists available at ScienceDirect

Bioorganic Chemistry

journal homepage: www.elsevier.com/locate/bioorg

Dual targeting of PTP1B and glucosidases with new bifunctional iminosugar inhibitors to address type 2 diabetes

Xhenti Ferhati[a,1], Camilla Matassini[a,1], Maria Giulia Fabbrini[a], Andrea Goti[a,b], Amelia Morrone[c], Francesca Cardona[a,b,*], Antonio J. Moreno-Vargas[d], Paolo Paoli[e,*]

[a] Department of Chemistry 'Ugo Schiff', University of Firenze, via della Lastruccia 3-13, Sesto Fiorentino, (FI), Italy
[b] Associated with Consorzio Interuniversitario Nazionale di ricerca in Metodologie e Processi Innovativi di Sintesi (CINMPIS), Italy
[c] Paediatric Neurology Unit and Laboratories, Neuroscience Department, Meyer Children's Hospital, and Department of Neurosciences, Pharmacology and Child Health. University of Florence, Viale Pieraccini n. 24, 50139 Firenze, Italy
[d] Departamento de Química Orgánica, Facultad de Química, Universidad de Sevilla, n/Prof. García González 1, E-41012 Sevilla, Spain
[e] Department of Experimental and Clinical Biomedical Sciences, University of Florence, Viale Morgagni 50, 50134 Florence, Italy

ARTICLE INFO

Keywords:
Type 2 diabetes
Bifunctional compounds
α-glucosidase inhibitors
PTP1B inhibitors
Iminosugars
Insulin-mimetic activity

ABSTRACT

The diffusion of type 2 diabetes (T2D) throughout the world represents one of the most important health problems of this century. Patients suffering from this disease can currently be treated with numerous oral anti-hyperglycaemic drugs, but none is capable of reproducing the physiological action of insulin and, in several cases, they induce severe side effects. Developing new anti-diabetic drugs remains one of the most urgent challenges of the pharmaceutical industry. Multi-target drugs could offer new therapeutic opportunities for the treatment of T2D, and the reported data on type 2 diabetic mice models indicate that these drugs could be more effective and have fewer side effects than mono-target drugs. α-Glucosidases and Protein Tyrosine Phosphatase 1B (PTP1B) are considered important targets for the treatment of T2D: the first digest oligo- and disaccharides in the gut, while the latter regulates the insulin-signaling pathway. With the aim of generating new drugs able to target both enzymes, we synthesized a series of bifunctional compounds bearing both a nitro aromatic group and an iminosugar moiety. The results of tests carried out both *in vitro* and in a cell-based model, show that these bifunctional compounds maintain activity on both target enzymes and, more importantly, show a good insulin-mimetic activity, increasing phosphorylation levels of Akt in the absence of insulin stimulation. These compounds could be used to develop a new generation of anti-hyperglycemic drugs useful for the treatment of patients affected by T2D.

1. Introduction

Non-insulin dependent diabetes mellitus (NIDDM), or T2D, is currently the most prevalent form of diabetes and the number of people affected by this pathology is continuously increasing worldwide [1]. Although non-genetic factors, such as obesity, a sedentary lifestyle and hypercaloric diets are the main causes of T2D, the disease also affects non-obese and physically active people, highlighting the importance of further research focussed on the onset mechanism. T2D is typically considered a pathology of the elderly, even though in the last century the number of diagnoses in men and women of middle age, or even in children began to rise [2]. In addition, it is a chronic pathology for which no definitive treatment is available. All current therapeutic options aim to stabilise the glycaemia of patients under the physiological range to avoid acute symptoms (hyperglycaemic peaks) and, in the long term, the risk of pathological complications [3]. Therapeutic options include oral anti-hyperglycaemic drugs such as metformin, gut amylase and α-glucosidase inhibitors, sulfonylureas, thiazolidinediones, glucagon-like peptide-1 receptor agonists, inhibitors of the degrading enzyme dipeptidyl peptidase 4, or, as a last resort, the injection of exogenous insulin [4]. No currently available drug is able to mimic the action of physiological insulin, therefore the search for new anti-diabetic drugs remains an important challenge.

Protein Tyrosine Phosphatase 1B (PTP1B) is one of the most promising targets for the treatment of T2D and metabolic syndrome. Administration of PTP1B inhibitors to diabetic mice models showed

* Corresponding authors at: Department of Experimental and Clinical Biomedical Sciences "Mario Serio", University of Florence, Viale Morgagni 50, 50134 Florence, Italy (Paolo Paoli), Department of Chemistry 'Ugo Schiff', University of Firenze, via della Lastruccia 3-13, Sesto Fiorentino (FI), Italy (Francesca Cardona).
E-mail addresses: francesca.cardona@unifi.it (F. Cardona), paolo.paoli@unifi.it (P. Paoli).
[1] These authors contributed equally to this work

https://doi.org/10.1016/j.bioorg.2019.03.053
Received 15 January 2019; Received in revised form 4 March 2019; Accepted 18 March 2019
Available online 22 March 2019
0045-2068/

normalization of glycaemia and loss of body weight in obese mice [5].

Since T2D can be managed by addressing different targets, an alternative approach based on bifunctional inhibitors could be more effective and could have fewer side effects.

Very recently, structurally complex polycyclic natural compounds isolated from different sources able to target both α-glucosidase and PTP1B were identified and characterized [6–12], suggesting that the use of such bifunctional drugs may delay the absorption of carbohydrates and, at the same time, enhance insulin sensitivity by modulating the insulin signalling pathway.

Several studies correlated insulin resistance with type 1 Gaucher Disease (GD1), the most prevalent lysosomal storage disorder, caused by an accumulation of glycosphingolipids in the lysosomes as an effect of hydrolytic enzyme malfunctioning (e.g. acid β-glucocerebrosidase (GCase), which is a β-glucosidase) [13]. GD1 patients show insulin resistance as well as other abnormalities in whole body metabolism [14–17], suggesting a connection between GD1 and T2D probably due to the influence of glycosphingolipids on insulin receptor functioning [18].

Since a β-glucosidase inhibitor has the potential to act as pharmacological chaperone rescuing the activity of the deficient enzyme in GD1 [19,20], an inhibitor addressing both β-glucosidase and PTP1B enzymes may act as a bifunctional drug to treat GD1 patients with diabetic complications.

With the aim of identifying new compounds with a dual activity to target T2D, we accessed new glycomimetics obtained by linking a phosphotyrosine mimetic group (namely a *p*-nitrophenyl moiety) and an iminosugar moiety. Among the many phosphotyrosine mimetic groups developed to target PTP1B inhibition, the *p*-nitrophenyl moiety proved to be effective due to its resemblance to the natural enzyme substrate [21] and, at the same time, it lacks of a net negative charge that hampers cell permeability and bioavailability [22]. The iminosugar moiety was introduced in order to impart α-/β- glucosidase inhibition and determine whether it could enhance PTP1B inhibition.

Iminosugars are carbohydrate analogues with a nitrogen atom replacing the endocylic oxygen of carbohydrates and are widely known as glycosidase inhibitors [23]. In particular, the pyrrolidine 1,4-dideoxy-1,4-imino-D-arabinitol (DAB-1, **1**) [24], *N*-alkylated deoxynojirimycin (DNJ) derivatives such as compound **2** (Fig. 1), [25] and the natural pyrrolizidine compound casuarine (**3**, Fig. 1) [26] have significant potential for treating T2D. The first oral drug for the treatment of diabetes based on an iminosugar compound, Miglitol (**4**, Fig. 1), is now commercially available. Miglitol inhibits the α-glucosidase enzymes in the brush border of the small intestine, delays glucose absorption and decreases postprandial hyperglycaemia [27].

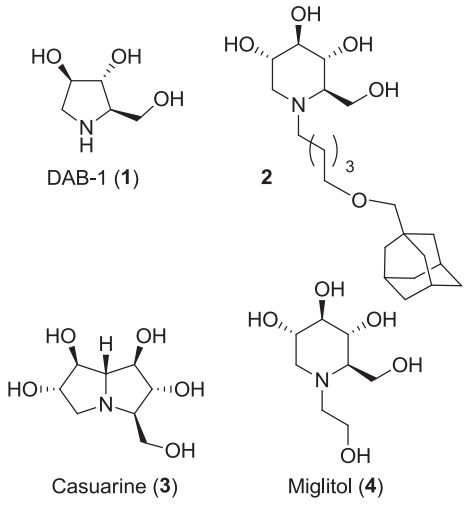

Fig. 1. Examples of iminosugars with potential application (**1–3**) or on the market (**4**) for T2D.

Due to a long-standing interest in the total synthesis of natural iminosugars and non-natural analogues with potential activity as glycosidase inhibitors, we screened a collection of iminosugars with different structures against PTP1B. The monocylic pyrrolidines **5a-j** [28–31] and piperidines **6a-f** [32,33], and bicyclic pyrrolizidines **7a-m** [34–38] and indolizidines **8a-e**) [39,40] shown in Figs. 2 and 3 were assayed.

Taking into consideration the activity shown by compound **5c** (see Discussion), we selected the pyrrolidine as the most promising structure for further development, because it is easier to synthesize and functionalize. We synthesized a series of new compounds characterized by the presence of the DAB-1 moiety (common to compound **5c** and to some of the bicyclic structures tested) linked to the nitroaromatic moiety with spacers of variable length (2, 3 and 4 carbon atoms) via a triazole (compounds **9–11**) or an amide (compounds **12–14**) moiety (Fig. 4).

These new iminosugar hybrids were assayed *in vitro* against PTP1B, and kinetic analyses were performed to evaluate their potency and mechanism of action. The activity of these bifunctional compounds was also evaluated towards commercial and human α- and β-glucosidases to assess their potential as dual inhibitors for the treatment of T2D. Finally, assays with HepG2 cells were carried out to evaluate their *ex vivo* effectiveness. The results of this multidisciplinary work are reported herein.

2. Results and discussion

2.1. Chemistry

2.1.1. Synthesis of bifunctional inhibitors

The synthesis of DAB-1 derivatives functionalized with an azido (compounds **17**, **22**, **23**) or an amino (compounds **24–26**) terminal moiety, suitable for further coupling with the nitro aromatic moiety, is shown in Scheme 1. The most straightforward approach was adopted for the 4-carbon atom linker, with the reaction of the benzylated DAB-1 **15** [29] with 1-azido-4-bromobutane **16** [41] under microwave heating in THF as a solvent, which produced compound **17** with an excellent 90% yield. For the 2- and 3-carbon atom linkers a different procedure was followed to avoid problems due to volatility and/or instability of low-molecular-weight azido derivatives. Compound **15** was reacted with 2-bromoethanol or 3-bromopropanol in THF at room temperature, to give the corresponding alcohols **18** and **19** with very good yields (85% and 94%, respectively). To introduce the terminal azido moiety, nucleophilic displacement with NaN_3 on the corresponding mesyl derivatives **20–21** was performed, leading to azides **22** and **23**. Compound **23** was produced with a 72% yield over two steps starting from alcohol **19**; the lower yield of compound **22** (6%) was ascribed to the formation of bicyclic spiro aziridinium by-products, which were visible in the crude reaction mixture. To overcome this problem, in the case of the 2-carbon atom linker, a direct Mitsunobu reaction with diphenyl phosphoryl azide (DPPA) on alcohol **19** was performed, giving a satisfactory 88% yield for compound **22**. The azido-amino reduction step was achieved either with catalytic hydrogenation under acidic conditions (for compound **26**), that also removed the *O*-benzyl protecting groups, or via the Staudinger reaction (compounds **24–25**), that allowed us to work with *O*-benzyl-protected derivatives in the subsequent conjugation step as shown in Scheme 2.

The *O*-benzyl protected azido derivatives **17**, **22** and **23** were reacted with 1-ethynyl-4-nitrobenzene in the presence of Cu(I) salts [42]. Since the reaction in THF gave only moderate yields at room temperature (53% for compound **27**), microwave (MW) irradiation and in-situ generated Cu(I) were performed for compounds **28** and **29**, leading to the much better yields of 87% and 92% respectively (Scheme 2). Treatment of **27–29** with BCl_3 in dichloromethane at room temperature allowed us to remove the *O*-benzyl groups without reducing the nitro

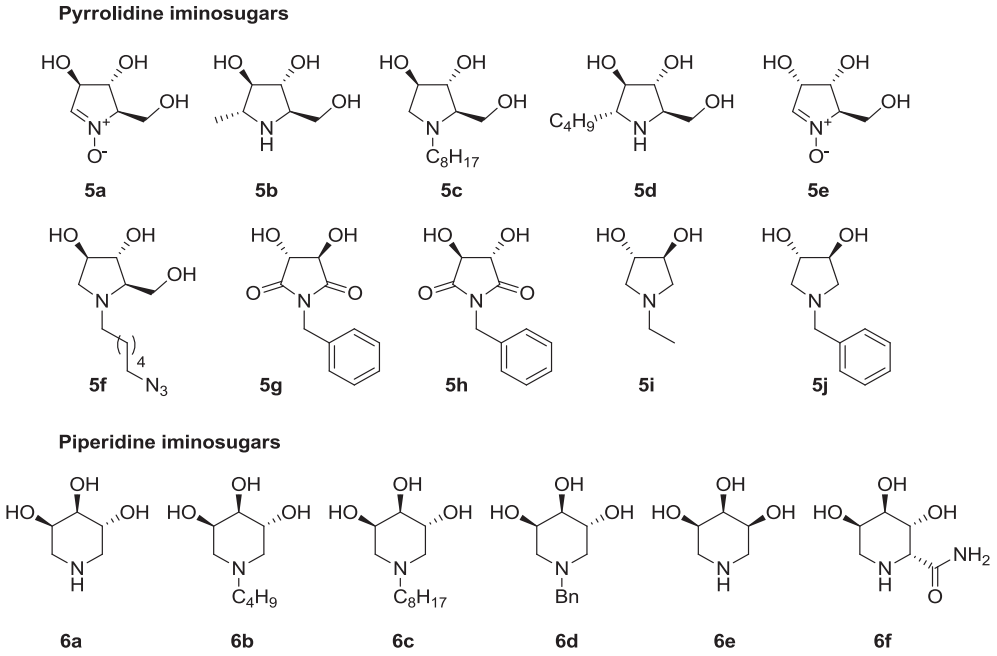

Fig. 2. Monocyclic iminosugars (pyrrolidines **5a-j** and piperidines **6a-f**) tested in this work as PTP1B inhibitors.

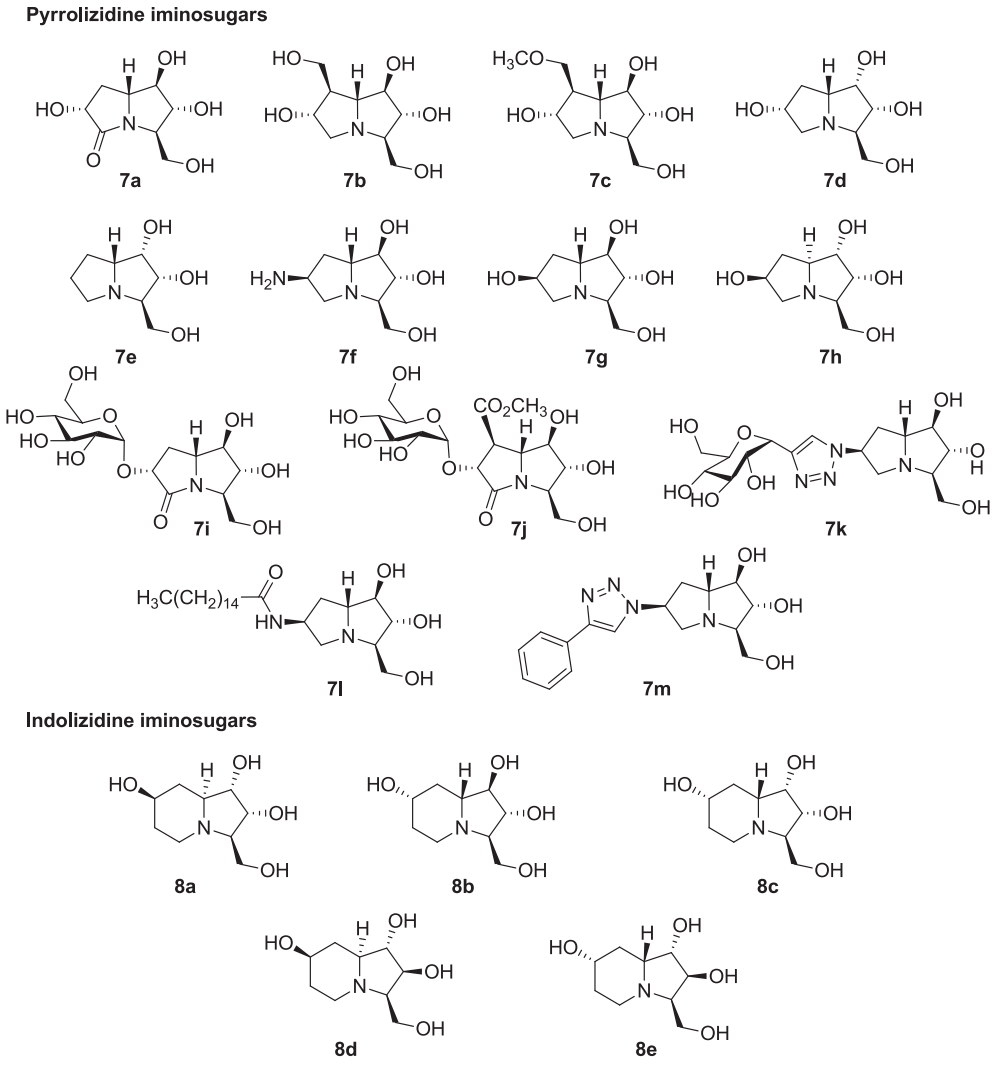

Fig. 3. Bicyclic iminosugars (pyrrolizidines **7a-m** and indolizidines **8a-e**) tested in this work as PTP1B inhibitors.

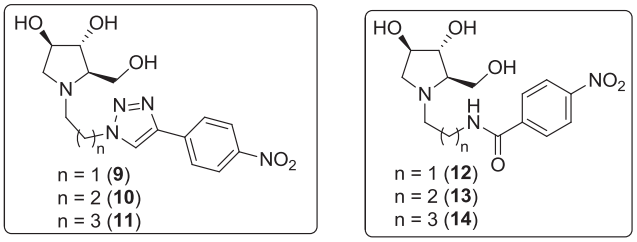

Fig. 4. Compounds **9–14** bearing the DAB-1 and the nitroaromatic moieties synthesized and tested in this work as bifunctional inhibitors.

moiety, as previously reported with the N−O bond of nitrones [43], producing the target compounds **9–11** with a yield of 63–85% after basic treatment with the resin Ambersep 900 OH in MeOH as a solvent. To prepare the amido derivatives **12–14**, direct acylation of **24–26** with 4-nitrobenzoyl chloride in pyridine as a solvent at room temperature produced compounds **13**, **34** and **35** with a 49–62% yield. With protected derivatives **34–35**, final treatment with BCl_3 in dichloromethane at room temperature followed by FCC (Flash Column Chromatography) with a basic eluent gave compounds **12** and **14** with yields of 70% and 85% (Scheme 2).

2.1.2. Synthesis of a multivalent bifunctional inhibitor

The concept of multivalency, defined as an increase in binding affinity when several bioactive units are simultaneously linked to a common scaffold [44], has been exploited with lectins [45–48]. Recently, research into the "multivalent effect" has also been carried out on enzymes [49–52]. In particular, impressive enhancement of activity was observed with multivalent iminosugars towards some glycosidases and several applications with therapeutically relevant enzymes have also been reported [53].

With the aim of investigating whether PTP1B could accommodate multivalent ligands bearing more than one iminosugar unit, we synthesized the new ligand **39** in which the nitro aromatic active moiety was linked to a trimeric DAB-1 moiety. Compound **39** was synthesized through a reaction of azido derivative **22** and propargylated TRIS **36** [54], as shown in Scheme 3. Compound **22** bearing a two-carbon atom spacer was chosen since this linker length proved to impart the best inhibitory activity towards PTP1B (vide infra). Copper catalyzed azido alkyne cycloaddition (CuAAC) between **22** and **36** under MW irradiation as described above gave compound **37** with a 68% yield. Subsequent acylation with *p*-nitrobenzoyl chloride, followed by *O*-benzyl deprotection with BCl_3 produced the trivalent derivative **39** with a good yield (Scheme 3).

2.2. Biology

2.2.1. Preliminary screening on PTP1B of the available iminosugars

Based on the observation that polyhydroxylated compounds are able to target both α-glucosidase and PTP1B [6–12], we envisaged that our iminosugars **5–8**, bearing several hydroxyl groups, could be similarly effective. Therefore, the whole collection of iminosugars **5–8** (Figs. 2 and 3) available in our laboratories was initially screened against PTP1B using a fixed inhibitor concentration (100 μM) as shown in Table 1. This preliminary evaluation showed that iminosugars **5–8** behave as moderate-to-good PTP1B inhibitors. Of all the compounds, **5c**, **6d**, **7g**, **7k-m** were the most potent, reducing PTP1B activity by up to 70%. Interestingly, by repeating the same test with a different phosphatase, namely the low molecular weight protein tyrosine phosphatase (LMW-PTP), we observed that the above-mentioned compounds were less active, suggesting a certain specificity for PTP1B over LMW-PTP.

It is worth noting that all the most active derivatives (30–40% residual activity) displayed the same absolute configuration at the pyrrolidine ring stereogenic centres. The results of this preliminary screening prompted us to choose compound **5c** for further functionalization, as it is one of the most active compounds against both PTP1B and glucosidases and much easier to synthesize and functionalize than other bicyclic pyrrolizidine iminosugars such as **7g** and **7k-m**.

2.2.2. Analysis of inhibitory properties of functionalized iminosugars *9–14* and *39*

Iminosugars **9–14** and **39** (Schemes 2 and 3) were analysed to evaluate their inhibitory power on the PTP1B enzyme. Preliminary screening carried out using both a fixed substrate and inhibitor (100 μM) concentration showed that compounds **9** and **13** were the most potent, whereas compounds **12** and **39** were weaker inhibitors. Finally, compounds **10**, **11** and **14** resulted completely inactive (Fig. 5).

These results suggest that the linker length plays a pivotal role in the activity of these compounds. The highest activity is shown by compound **13**, with a five-atom linker (amide bond included) between the DAB-1 moiety and the nitro aromatic ring. A shorter linker (four atoms, as in compound **12**) reduces inhibitory potency, while a longer one (six or seven atoms, as in compounds **10** and **11**) results in a complete loss of activity. Interestingly, the triazole based compound **9** and the amide based compound **13** show a similar inhibitory profile and both have a five-atom spacer between the two bioactive moieties, demonstrating that the triazole moiety is able to replace the amide bond without detrimental effects on biological activity, as expected since the 1,2,3-triazole moiety is well known as an amide bond isostere [55,56].

To confirm these results, we calculated the IC_{50} values of active

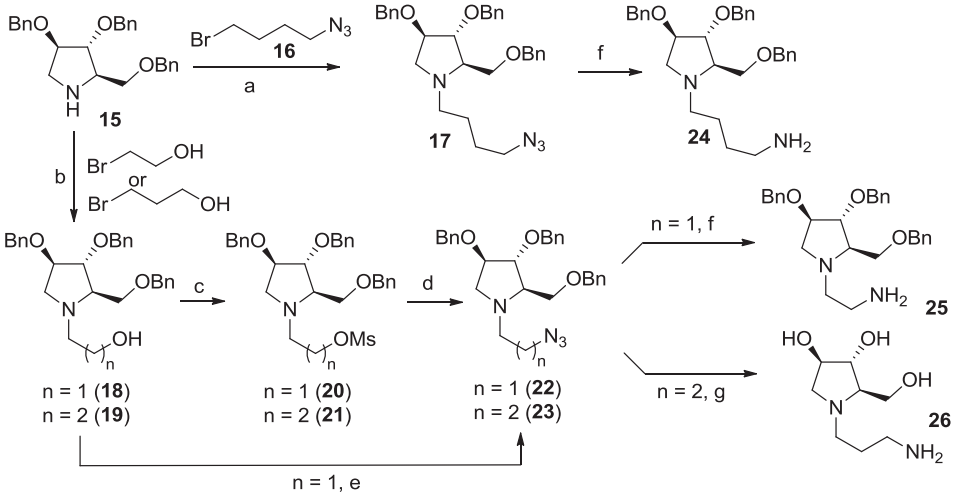

Scheme 1. Synthesis of key azido and amino DAB-1 based intermediates **24–26**. Reaction conditions: (a) NEt_3, THF, MW 150 °C, 4 h, 90%; (b) NEt_3, THF, r.t., 3 days, 85% for **18**, 94% for **19**; (c) MsCl, NEt_3, CH_2Cl_2, r.t., 2 h, 25% for **20**, 77% for **21**; (d) NaN_3, 18-crown 6 ether, CH_3CN, reflux, 5 h, 25% for **22**, 94% for **23**; (e) DPPA, PPh_3, DIAD, THF, r.t., 88% for **22**; (f) PPh_3, H_2O, THF, reflux, 16 h, 84% for **24**, 63% for **25**; (g) H_2, Pd/C, HCl, MeOH, r.t., 2 days, 86%.

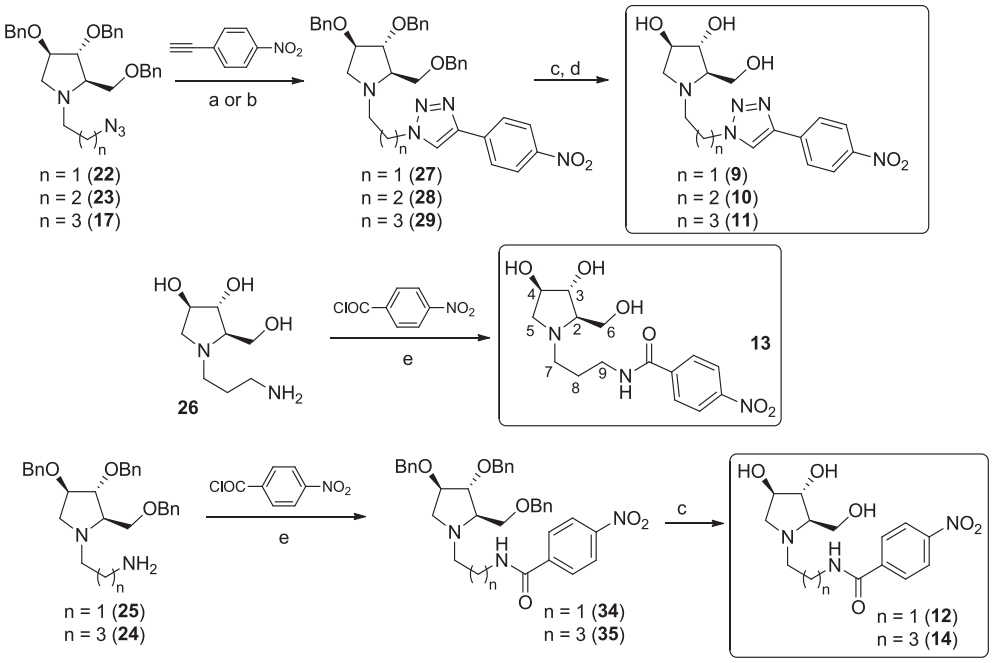

Scheme 2. Synthesis of the target triazole-derivatives **9–11** and amide derivatives **12–14**. Reaction conditions: (a) CuI, DIPEA, THF, r.t., 2 h, 53% for **27**; (b) $CuSO_4$, sodium ascorbate, THF, H_2O, MW, 80 °C, 45 min, 87% for **28**, 92% for **29**; (c) BCl_3, CH_2Cl_2, r.t., 15–18 h, 63–85% for **9–11**, 70% for **12** and 85% for **14**; (d) Ambersep 900 OH, MeOH, r.t., 30 min, quantitative; e) Py, r.t., 22–40 h, 49% for **13**, 56% for **34**, 62% for **35**.

compounds, including compound **5c** (data obtained are reported in Table 2). Compound **13** was the most potent of the screened molecules, with an IC_{50} value of 31 µM, a value equivalent to half of that calculated for compound **5c**. Compounds **9**, **12** and **39** were weaker inhibitors, with IC_{50} values of 103, 180 and 119 µM, respectively.

To gain insight into the mechanism of action of the best nitrophenyl substituted inhibitors, compounds **9** and **13** (see Fig. 4), the dependence of the main kinetic parameters, K_m and V_{max}, on inhibitor concentration was investigated. Data obtained were analysed using the Lineweaver-Burk plot. It was found that compounds **9** and **13** behave as non-competitive inhibitors (Fig. 6, see also Fig. S49 of the Supporting Information), as demonstrated by the fact that the compounds have a very limited effect on K_m while causing the reduction of V_{max} (see Fig. S47 and S48 of the Supporting Information). By using an appropriate equation (see Materials and Methods section), we calculated the Ki values for each compound, which resulted 153 ± 41 µM and 32 ± 3 µM for compounds **9** and **13**, respectively.

2.2.3. Analysis of inhibitory properties of control compounds

To verify the role played by the iminosugar moiety in PTP1B inhibition, we also prepared and evaluated compounds **40** and **41** as control systems (Fig. 7). Compared to compound **13**, compound **40** [57] lacks the iminosugar moiety DAB-1 and compound **41** lacks the two hydroxy groups and the hydroxymethyl on the pyrrolidine ring.

We found that both compounds are inactive, demonstrating that both the pyrrolidine group and the hydroxyl functionalities are essential in imparting inhibitory activity to the final compound towards PTP1B (Fig. S50 of the Supporting Information).

2.2.4. Effect of compounds on α-glucosidases

The inhibition of amylase and intestinal α-glucosidase prevents the digestion of carbohydrates, thus representing a second mechanism through which our compounds could act as anti-diabetic drugs. Synthetic drugs that inhibit α-glucosidase are widely used in the clinic to treat T2D mellitus, causing a reduction in postprandial blood glucose and insulin levels [58]. Therefore, commercial porcine pancreatic amylase was chosen as a model and compounds **5c, 9–14** and **39** were assayed towards this enzyme using *p*-nitrophenyl-α-D-glucopyranoside as a synthetic substrate. We did not find these compounds to be capable of inhibiting this enzyme. However, a good inhibitory profile was found towards α-glucosidase from *Saccharomyces cerevisiae* and towards amyloglucosidase from *Aspergillus niger* for compounds **5c** and **13**,

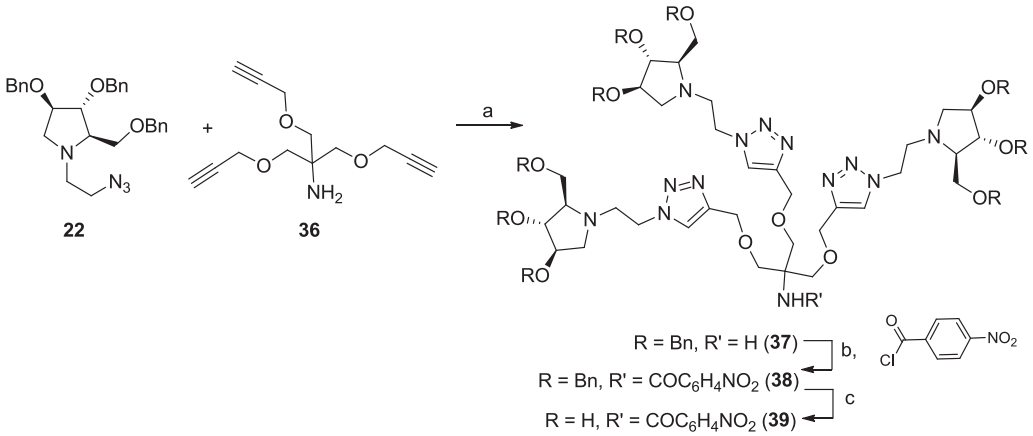

Scheme 3. Synthesis of trivalent derivative **39**. Reaction conditions: (a) $CuSO_4$, sodium ascorbate, THF, H_2O, MW, 80 °C, 45 min, 68% of **37**; (b) DIPEA, CH_2Cl_2, r.t., 2 days, 85% of **38**; (c) BCl_3, CH_2Cl_2, r.t., 18 h, 95% of **39**.

Table 1
Preliminary enzymatic assays. Tests were carried out on PTP1B and LMW-PTP by using a fixed inhibitor concentration (100 μM) and a fixed substrate concentration (2.5 mM). Data reported in the Table represent the mean ± S.E.M. (n = 3).

	Compounds	Residual activity (%)	
		PTP1B	LMW-PTP
Pyrrolidiness	Ctr	100	100
	5a	141 ± 1	116 ± 3
	5b	84 ± 15	82 ± 2
	5c	**34 ± 9**	71 ± 1
	5d	89 ± 8	81 ± 2
	5e	92 ± 3	109 ± 2
	5f	110 ± 6	86 ± 1
	5g	82 ± 4	147 ± 2
	5h	73 ± 1	154 ± 14
	5i	62 ± 2	80 ± 2
	5j	64 ± 4	96 ± 5
Piperidines	**6a**	61 ± 12	78 ± 2
	6b	68 ± 8	78 ± 1
	6c	82 ± 7	103 ± 5
	6d	**47 ± 5**	78 ± 16
	6e	84 ± 7	86 ± 2
	6f	76 ± 3	98 ± 3
Pyrrolizidines	**7a**	83 ± 7	102 ± 5
	7b	67 ± 3	85 ± 1
	7c	60 ± 2	112 ± 8
	7d	73 ± 7	102 ± 2
	7e	57 ± 8	62 ± 3
	7f	63 ± 4	74 ± 4
	7g	**38 ± 6**	68 ± 4
	7h	83 ± 2	103 ± 2
	7i	103 ± 7	116 ± 3
	7j	55 ± 10	118 ± 6
	7k	**31 ± 9**	88 ± 8
	7l	**40 ± 3**	132 ± 3
	7m	**38 ± 2**	120 ± 4
Indolizidines	**8a**	134 ± 2	135 ± 1
	8b	68 ± 4	85 ± 5
	8c	131 ± 6	132 ± 2
	8d	82 ± 12	102 ± 5
	8e	113 ± 5	109 ± 3

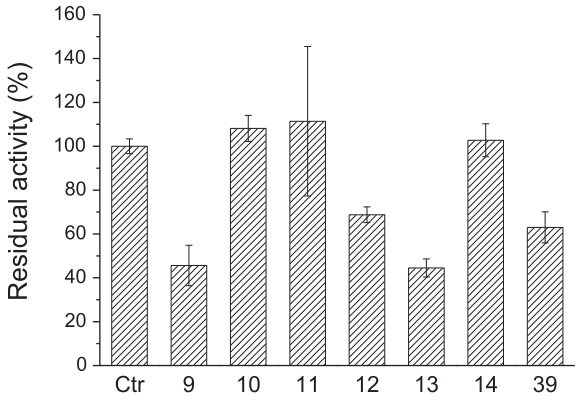

Fig. 5. Preliminary enzymatic assay on PTP1B. Tests were carried out in 3,3-dimethylglutarate buffer pH 7.0 containing 0.1 mM DTT and 1 mM EDTA, in the presence of a fixed substrate concentration (2.5 mM, corresponding to the Km value of the enzyme) and a fixed inhibitor concentration (100 μM). Data reported in the figure represent the mean value ± S.E.M (n = 3).

which are the best PTP1B inhibitors we have analysed. Preliminary screening carried out using a fixed inhibitor concentration (1 mM) showed the inhibition percentage of both α-glucosidases to be higher than 90%. Upon IC_{50} determination, we found that compounds **5c** and **13** are both good inhibitors of amyloglucosidase from *Aspergillus niger* (IC_{50} = 4.1 μM and 4.0 μM, respectively) and good-to-moderate inhibitors of α-glucosidase from *Saccharomyces cerevisiae* (IC_{50} = 6.4 μM and 25.0 μM, respectively, see Table 3).

Selectivity towards different α-glucosidases is an important issue. Compounds **5c**, **9–14** and **39** were thus evaluated as lysosomal α-glucosidase inhibitors in human lymphocytes homogenate [59,60]. Compounds **9–12** and **14** inhibited lysosomal α-glucosidase (82–94%) at 1 mM and their IC_{50} values were subsequently determined by measuring human enzyme activity at different iminosugar concentrations (Table 4). To our delight, compounds **13** and **5c**, the best PTP1B inhibitors, were only weak α-glucosidase inhibitors (percentage of inhibition around 40%).

In the development of novel candidates as potential antidiabetic agents, the inhibition of lysosomal α-glucosidase is undesirable as it can result in the accumulation of non-hydrolyzed substrate in the lysosome, with clinical manifestations similar to those observed in Pompe Disease, a lysosomal storage disorder caused by a mutation in the gene encoding for lysosomal α-glucosidase (*GAA*) [61].

2.2.5. Effect of compounds on human lysosomal β-glucosidase (GCase)

Since a lysosomal β-glucosidase inhibitor has the potential to act as pharmacological chaperone rescuing the activity of the deficient enzyme in Gaucher Disease, we tested the synthesized compounds towards acid β-glucosidase (glucocerebrosidase, GCase) from human leukocytes homogenates. We found that a residual enzymatic activity no higher than 18% was observed for the whole set of compounds (except for the trivalent derivative **39**) when assayed at 1 mM concentration, as shown in Fig. 8. Since compounds **9** and **13** are also good PTP1B inhibitors, further investigations of their GCase inhibitory profile/kinetics would be of particular interest in view of the potential application of these compounds as bifunctional PTP1B/GCase inhibitors/chaperones in the treatment of T2D related to Gaucher disease.

In this regard, both therapeutic actions (inhibitory and chaperone) may be relevant. While a pharmacological chaperone for GCase rescues the activity of the endogenous enzyme, which is deficient in the pathology, it can also stabilize the exogenous GCase enzyme in patients treated with enzyme replacement therapy (ERT). From the existing literature, it is not clear if the onset of T2D is related to Gaucher Disease (even untreated) or only to Gaucher Disease patients treated with Enzyme Replacement Therapy (ERT) [18]. Metabolic abnormalities are apparent in Gaucher Disease but the administration of the recombinant enzyme to reduce glucosylceramide levels in patients seems to have its own metabolic consequences, such as peripheral insulin resistance [15]. This may be due to reductions of glucosylceramide levels *per se* or secondary glycosphingolipids alterations, such as transient increases in ceramide as the excess glucosylceramide passes through the catabolic pathways [15]. Inhibition of GCase (the enzyme responsible for the conversion of glucosylceramide into glucose and ceramide) could avoid accumulation of ceramide inside the cells, a metabolite that is able to impair the translocation of Akt and promote Akt dephosphorylation by PP2A, thereby resulting in Akt inactivation [62].

2.2.6. Ex vivo assay

In order to evaluate whether compounds **13** and **9** possessed insulin-mimetic activity, further tests using HepG2 cells were performed. Cells were starved for 20 h and then treated with compound **9** or **13**, or stimulated with 10 nM insulin. The proteins of extracts were separated by SDS-PAGE and transferred to PVDF membrane by western blot. Membranes were probed with specific antibodies to evaluate levels of the phosphorylate form of Akt (Fig. 9). As expected, after insulin stimulation, a great increase in the phosphorylation level of Akt was observed. An increase in Akt phosphorylation was already detectable after 15 min incubation with both compounds, suggesting that **9** and **13** possess insulin mimetic activity.

Interestingly, no increase in the Akt phosphorylation level was observed on HepG2 cells treated with 100 μM of compound **5c** (data not

Table 2
IC_{50} values for compounds **5c**, **9**, **12**, **13** and **39** towards PTP1B. To determine the IC_{50} values, we calculated residual activity of PTP1B in the presence of increasing inhibitor concentrations and a fixed substrate concentration (2.5 mM). Each assay was carried out in triplicate.

Compound	9	12	13	39	5c
IC_{50} (μM)	103 ± 4	180 ± 4	31 ± 2	119 ± 9	66 ± 2

shown). This finding suggested that compound **5c** does not possess an evident insulin-mimetic activity, thereby confirming that the presence of the nitro aromatic moiety is essential to confer an insulin-mimetic activity to compounds **9** and **13.**

To date, we can only speculate on the mechanisms of the *ex vivo* effect of compounds **9** and **13**, which could be due to PTP1B inhibition, or to β-glucosidase inhibition.

3. Conclusions

The development of effective drugs for the treatment of T2D or insulin resistance is one of the most important goals of pharmaceutical companies. A growing body of evidence shows that multi-target drugs could be good alternatives to traditional therapies, offering the possibility of simultaneously controlling the activity of different targets, without the risk of generating undesirable secondary effects.

Protein Tyrosine Phosphatase 1B (PTP1B) is one of the most promising targets for the treatment of T2D and metabolic syndrome. On the other hand, α-glucosidase inhibitors have the potential to be developed as oral anti-hyperglycaemic drugs.

In this work, we show that our new bifunctional inhibitors, obtained by linking an iminosugar moiety with a phosphotyrosine mimetic group, are able to target both PTP1B and α-glucosidases.

The privileged iminosugar moiety (a polyhydroxylated pyrrolidine) was selected on the basis of a preliminary screening towards PTP1B of more than 30 iminosugars with different structures. We synthesized a

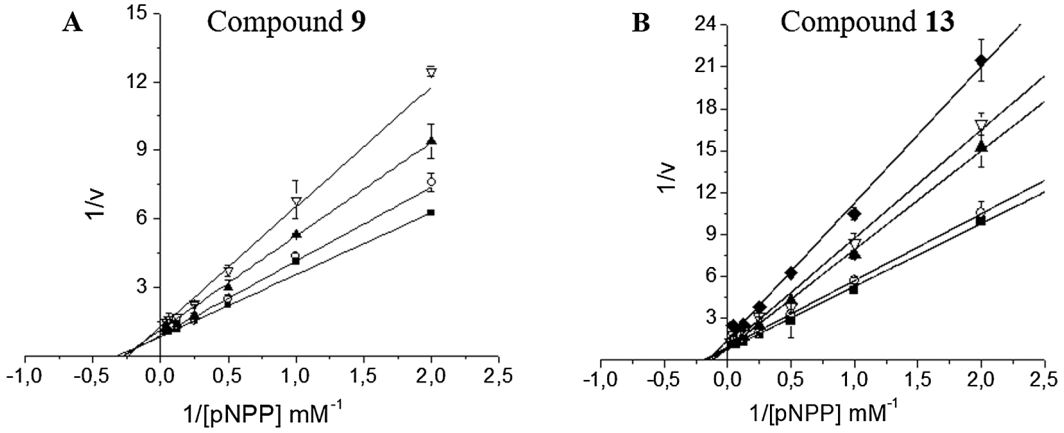

Fig. 6. Double reciprocal plots for compounds **9** (A) and **13** (B). pNPP (*p*-nitrophenylphosphate) is employed as a synthetic substrate. (A) The concentration of compound **9** are: ■, 0 μM; ○, 80 μM; ▲, 100 μM; ▽, 120 μM. Data reported in the figures represent the mean values ± S.E.M. (n = 3). (B) The concentration of compound **13** are: ■, 0 μM; ○, 15 μM; ▲, 25 μM; ▽, 35 μM; ♦, 45 μM; data reported in the figures represent the mean values ± S.E.M. (n = 3).

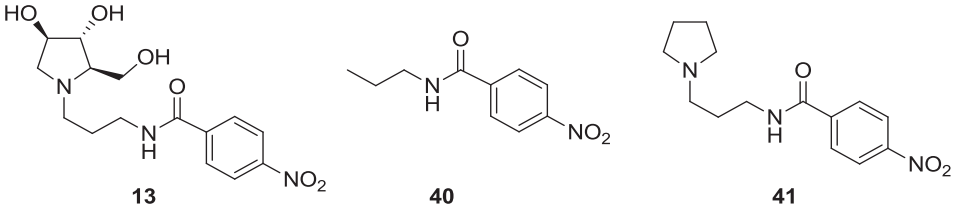

Fig. 7. Chemical structure of compounds **13**, **40**, and **41**. Compounds **40** and **41** were used as control compounds to verify the importance of the iminosugar moiety in PTP1B inhibition.

Table 3
IC_{50} values determined by measuring the residual activity of α-glucosidases in the presence of increasing inhibitor concentration for iminosugars **5c** and **13**.

Compound	Amyloglucosidase from *Aspergillus niger*, IC_{50}, μM	α-Glucosidase from *Saccharomyces cerevisiae*, IC_{50}, μM
5c	4.1	6.4
13	4.0	25.0

Table 4
Inhibition of lysosomal α-glucosidase (in an extract from human lymphocytes) by compounds **5c**, **9–14** and **39**. IC_{50} values determined for percentages of inhibition higher than 80% by measuring the residual activity of α-glucosidase in the presence of increasing inhibitor concentration. For each compound, we used at least 10 different inhibitor concentrations. Each assay was carried out in triplicate.

Compound	5c	9	10	11	12	13	14	39
IC_{50} (μM)	———[a]	240 ± 10	210 ± 10	170 ± 5	250 ± 10	———[a]	170 ± 10	———[a]

[a] Compounds **5c**, **13** and **39** showed percentage of inhibition lower than 80% at 1 mM inhibitor concentration.

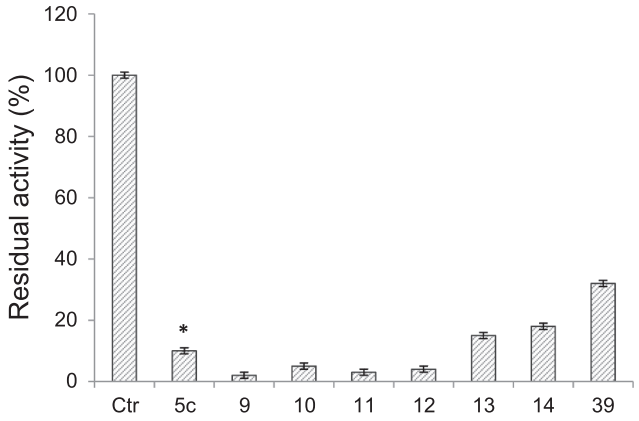

Fig. 8. Residual activity of β-glucosidase (GCase) in an extract from human leukocytes isolated from healthy donors, incubated with 1 mM iminosugars **5c**, **9–14** and **39**. *The percentage of inhibition and the IC_{50} value (108 ± 14 μM) are reported in Ref. 28, where the same assay conditions were employed.

series of six novel compounds **9–14** in which the iminosugar moiety and the nitro aromatic phosphotyrosine mimetic group were connected through linkers that differ in nature (amide or a triazole ring) and length (2, 3 or 4 carbon atoms), and the trivalent compound **39**. Some of the new compounds (namely **9**, **12**, **13**, and **39**), maintained the ability to inhibit the PTP1B enzyme with IC_{50} values that ranged between 30 and 180 μM. Analysis of kinetic parameters showed that compounds **9** and **13**, the best PTP1B inhibitors bearing the nitrophenyl moiety, behave as non-competitive inhibitors (Fig. 6). Moreover, the presence of the iminosugar moiety was demonstrated to be essential in imparting inhibitory activity towards PTP1B, since compounds **40** and **41,** lacking the polyhydroxylated pyrrolidine moiety, did not show any inhibitory activity. Our best PTP1B inhibitors **13** and **5c** were also assayed towards commercial α-glucosidases, namely α-glucosidase from *Saccharomyces cerevisiae* and amyloglucosidase from *Aspergillus niger*, and moderate to good inhibition was found for both compounds (IC_{50} values ranging from 4 to 25 μM). These results pave the way for a new generation of bifunctional PTP1B/α-glucosidase inhibitors. Undesired inhibition of lysosomal α-glucosidase was negligible for both compounds.

Furthermore, *ex vivo* tests carried out on HepG2 cells demonstrated that the new nitrobenzene iminosugar hybrids **9** and **13** show a good insulin-mimetic activity, increasing phosphorylation levels of Akt also in the absence of insulin stimulation, while the iminosugar **5c** was not active in the *ex vivo* assay.

To the best of our knowledge, examples of iminosugar-based PTP1B inhibitors are unprecedented, thus this study represents proof of concept for the possible use of iminosugars as new bifunctional drugs in the treatment of T2D. Work is underway to improve the potency of inhibitors towards the selected enzymatic targets and to elucidate the mechanism underlying their *ex vivo* activity.

4. Materials and methods

4.1. Chemistry

Commercial reagents were used as received. All reactions were carried out under magnetic stirring and monitored by TLC on 0.25 mm silica gel plates (Merck F_{254}). Column chromatographies were carried out on Silica Gel 60 (32–63 μm) or on silica gel (230–400 mesh, Merck). Yields refer to spectroscopically and analytically pure compounds unless otherwise stated. ^{1}H NMR spectra were recorded on a Varian Mercury-400 or on a Varian INOVA 400 instrument at 25 °C. ^{13}C NMR spectra were recorded on a Varian Gemini-200 or on a Varian Gemini-300. Chemical shifts are reported relative to TMS (^{1}H: δ = 0.00 ppm) and $CDCl_3$ (^{13}C: δ = 77.0 ppm). Integrals are in accordance with assignments, coupling constants are given in Hz. For detailed peak assignments 2D spectra were measured (COSY, HSQC, NOESY, and NOE as necessary). Small scale microwave assisted syntheses were carried out in a CEM Discover microwave apparatus for synthesis with an open reaction vessel and an external surface sensor. IR spectra were recorded with a BX FT-IR Perkin-Elmer System spectrophotometer. ESI-MS spectra were recorded with a Thermo Scientific™ LCQ Fleet Ion Trap Mass Spectrometer. HRESI-MS spectra were recorded with a Thermo Scientific™ Orbitrap Elite or with an ABSCIEX Triple TOF® 5600$^+$ instrument. Optical rotation measurements were performed on a JASCO DIP-370 polarimeter.

Synthesis of (2*R*,3*R*,4*R*)-1-(4-azidobutyl)-3,4-bis(benzyloxy)-2-[(benzyloxy)methyl] pyrrolidine (17): A solution of pyrrolidine **15** [29] (86 mg, 0.21 mmol) in THF (2 mL) was prepared in a MW vial, and NEt_3 (60 μL, 0.42 mmol) and 1-azido-4-bromobutane **16** [41] (86 mg, 0.48 mmol) were added. The reaction mixture was heated in MW reactor at 150 °C for 45 min until a TLC analysis showed the disappearance of the starting material and the formation of a new product. The solvent was removed under reduced pressure and the crude was purified by FCC (CH_2Cl_2/Et_2O 100:1) affording pure **17** (93 mg, 0.19 mmol) with a 90% yield. **[α]$_D^{25}$** = −31.1 (c = 0.94, $CHCl_3$). ^{1}H **NMR** (400 MHz, $CDCl_3$) δ ppm = 7.35–7.25 (m, 15H, Ar), 4.55–4.42 (m, 6H, O-$\underline{CH_2}$-Ph), 3.92 (d, *J* = 5.4 Hz, 1H, H-4), 3.86 (d, *J* = 4.3 Hz, 1H, H-3), 3.54 (m, 2H, H-6), 3.26 (m, 2H, H-10), 3.20 (d, *J* = 10.5 Hz, 1H, Ha-5), 2.87 (m, 1H, Ha-7), 2.72 (q, *J* = 5.2 Hz, 1H, H-2), 2.55 (dd, *J* = 10.5, 5.1 Hz, 1H, Hb-5), 2.36 (m, 1H, Hb-7), 1.66–1.52 (m, 4H, H-8, H-9). **^{13}C NMR** (50 MHz, $CDCl_3$) δ ppm = 138.5, 138.4 (s, 3C, Ar), 128.3, 127.6 (d, 15C, Ar), 85.6 (d, 1C, C-3), 81.8 (d, 1C, C-4), 73.2, 71.1 (t, 4C, O-$\underline{CH_2}$-Ph, C-6), 69.3 (d, 1C, C-2), 57.2 (t, 1C, C-5), 54.8 (t, 1C, C-7), 51.4 (t, 1C, C-10), 26.8–25.4 (t, 2C, C-8, C-9). **IR** ($CDCl_3$) ν = 3032, 2934, 2865, 2808, 2099, 1496, 1453, 1365, 1350, 1282, 1259, 1098, 1076 cm^{-1}. **MS-ESI** (*m*/*z*, %) = 501.28 (MH^+, 100), 523.28 (MNa^+, 62).

Synthesis of 2-{(2*R*,3*R*,4*R*)-3,4-bis(benzyloxy)-2-[(benzyloxy) methyl] pyrrolidin-1-yl}ethanol (18): [63,64] To a pyrrolidine **15** [29]; solution (82 mg, 0.20 mmol) in THF (3 mL), NEt_3 (141 μL, 1.00 mmol) and 2-bromoethanol (85 μL, 1.22 mmol) were added. The reaction mixture was stirred at room temperature for 3 days until a TLC

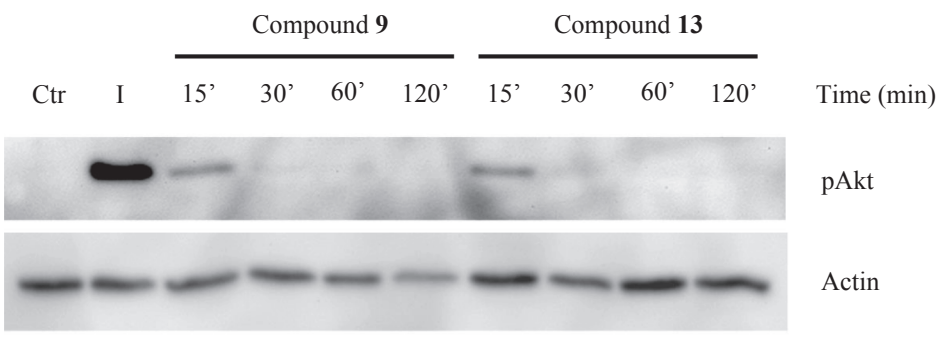

Fig. 9. Effect of compound 9 and 13 on insulin signalling pathway. HepG2 cells were starved and then stimulated with 10 nM insulin for 15 min, or treated with compound **9** and **13** for increasing times. At the end of each interval time, cells were lysed and analysed to evaluate phosphorylation levels of Akt using specific antibodies. The final concentration of compounds **9** and **13** in the test was 42 μM.

analysis (CH_2Cl_2/MeOH 30:1) showed the disappearance of the starting material (Rf = 0.43) and the formation of a new product (Rf = 0.81). After evaporation under reduced pressure, the crude was purified by FCC (AcOEt/PE 1:1) affording pure **18** (Rf = 0.30, 75 mg, 0.17 mmol, 85% yield) as a yellow oil. $[\alpha]_D^{25} = -20.3$ (c = 0.92 in $CHCl_3$). **^{1}H NMR** (400 MHz, CDCl3): δ = 7.35–7.26 (m, 15H, H-Ar), 4.55–4.42 (m, 6H, O-$\underline{CH_2}$-Ph), 3.99–3.97 (m, 1H, H-4), 3.89 (dd, J = 3.6, 1.2 Hz, 1H, H-3), 3.64–3.48 (m, 4H, H-7, H-8), 3.25 (d, J = 10.4 Hz, 1H, Ha-5), 3.06 (ddd, J = 12.9, 9.1, 4.7 Hz, 1H, Ha-6), 2.88 (dd, J = 9.6, 5.6 Hz, 1H, H-2), 2.67 (dd, J = 10.4, 5.2 Hz, 1H, Hb-5), 2.58 (dt, J = 12.6, 3.8 Hz, 1H, Hb-6).

Synthesis of 2-{(2*R*,3*R*,4*R*)-3,4-bis(benzyloxy)-2-[(benzyloxy) methyl] pyrrolidin-1-yl}propan-1-ol (19): [64] To a solution of **15** [29] (132 mg, 0.33 mmol) in 6 mL of THF, NEt_3 (230 µL, 1.65 mmol) and 3-bromo-1-propanol (179 µL, 1.98 mmol) were added. The reaction mixture was stirred at room temperature for 3 days until a TLC analysis (CH_2Cl_2/MeOH 10:1) showed the disappearance of the starting material (R_f = 0.51) and the formation of a new product (R_f = 0.85). After evaporation under reduced pressure, the crude was purified by FCC (AcOEt/PE 1:1) affording pure **19** (R_f = 0.30, 143 mg, 0.31 mmol, 94% yield) as a yellow oil. $[\alpha]_D^{24} = -39.1$ (c = 0.47 in $CHCl_3$). **^{1}H NMR** (400 MHz, $CDCl_3$): δ = 7.34–7.24 (m, 15H, H-Ar), 4.56–4.48 (m, 6H, O-$\underline{CH_2}$-Ph), 3.93 (d, J = 4.8 Hz, 1H, H-4), 3.82–3.77 (m, 3H, H-9 and H-3), 3.63 (dd, J = 9.7, 5.8 Hz, 1H, Ha-6), 3.55 (dd, J = 9.8, 6.4 Hz, 1H, Hb-6), 3.45 (d, J = 10.8 Hz, 1H, Ha-5), 3.14 (td, J = 11.7, 3.9 Hz, 1H, Ha-7), 2.73 (q, J = 5.2 Hz, 1H, H-2), 2.64 (dt, J = 12.2, 3.9 Hz, 1H, Hb-7), 2.50 (dd, J = 10.8, 4.7 Hz, 1H, Hb-5), 1.94–1.82 (m, 1H, Ha-8), 1.56–1.49 (m, 1H, Hb-8). **^{13}C NMR** (50 MHz, $CDCl_3$): δ = 138.3, 138.2, 138.1 (s, 3C, C-Ar), 128.3–127.5 (d, 15C, C-Ar), 85.3 (d, 1C, C-3), 81.4 (d, 1C, C-4), 73.3, 71.4, 71.2, 70.9 (t, 4C, C-Bn and C-6), 69.7 (d, 1C, C-2), 64.0 (t, 1C, C-9), 56.7 (t, 1C, C-5), 55.2 (t, 1C, C-7), 29.3 (t, 1C, C-8). **IR** ($CDCl_3$): ν = 3312, 3066, 3032, 2923, 2861, 1496, 1453, 1366, 1333, 1282, 1208, 1100, 1071, 1028 cm^{-1}. **MS-ESI** (m/z, %) = 484.33 (MNa^+, 100), 462.30 (MH^+, 74).

Synthesis of 2-{(2*R*,3*R*,4*R*)-3,4-bis(benzyloxy)-2-[(benzyloxy) methyl] pyrrolidin-1-yl}ethyl methanesulfonate (20): A solution of alcohol **18** (130.0 mg, 0.29 mmol) in anhydrous CH_2Cl_2 (5 mL) was stirred under nitrogen atmosphere and cooled at 0 °C. NEt_3 (121 µL, 0.87 mmol) and MsCl (29 µL, 0.38 mmol) were added and the reaction mixture was left to reach room temperature and stirred for 2 h. The mixture was transferred to a separatory funnel and washed with H_2O. The aqueous layer was then extracted with CH_2Cl_2 (3 × 15 mL) and the combined organic layers were dried over Na_2SO_4. The solvent was evaporated under a vacuum and the crude was purified by FCC (AcOEt/PE 1:1), leading to pure **20** (38.1 mg, 0.072 mmol) with a 25% yield. Due to the instability of compound **20** (see main text), it was impossible to obtain a complete characterization of this product. The ^{1}H NMR spectrum is reported below. **^{1}H NMR** (200 MHz, CDCl3) δ ppm = 7.38–7.26 (m, 15H), 4.53–4.35 (m, 7H), 4.26 (m, 1H), 3.94 (d, J = 5.0 Hz, 1H), 3.80 (d, J = 4.2 Hz, 1H), 3.54 (d, J = 5.8 Hz, 2H), 3.29 (m, 2H), 2.96 (s, 3H), 2.73 (m, 3H).

Synthesis of 2-{(2*R*,3*R*,4*R*)-3,4-bis(benzyloxy)-2-[(benzyloxy) methyl] pyrrolidin-1-yl}propyl methanesulfonate (21): A solution of alcohol **19** (34 mg, 0.073 mmol) in anhydrous CH_2Cl_2 (2 mL) was stirred under nitrogen atmosphere and cooled at 0 °C. NEt_3 (121 µL, 0.87 mmol) and MsCl (29 µL, 0.38 mmol) were added and the reaction mixture was left to reach room temperature and stirred for 2 h. The mixture was transferred to a separatory funnel and washed with H_2O. The aqueous layer was then extracted with CH_2Cl_2 (3 × 15 mL) and the combined organic layers were dried over Na_2SO_4. The solvent was evaporated under a vacuum and the crude was purified by FCC (AcOEt/PE 1:2), affording pure **21** (30.2 mg, 0.056 mmol) with a 77% yield. $[\alpha]_D^{25} = -16.7$ (c = 1.21, $CHCl_3$). **^{1}H NMR** (400 MHz, $CDCl_3$) δ ppm = 7.38–7.23 (m, 15H, Ar), 4.61–4.39 (m, 6H, O-$\underline{CH_2}$-Ph), 4.27 (m, 2H, H-9), 3.94 (d, J = 5.3 Hz, 1H, H-4), 3.85 (d, J = 3.9 Hz, 1H, H-3), 3.54 (m, 2H, H-6), 3.18 (d, J = 10.2 Hz, 1H, Ha-5), 5.98 (dt, J = 12.5, 8.1 Hz, 1H, Ha-7), 2.91 (s, 3H, Me), 2.74 (m, 1H, H-2), 2.56 (dd, J = 10.2, 5.3 Hz, 1H, Hb-5), 2.46 (m, 1H, Hb-7), 1.91 (m, 2H, H-8). **^{13}C NMR** (50 MHz, $CDCl_3$) δ ppm = 138.3–138.1 (s, 3C, Ar), 128.3–127.7 (d, 15C, Ar), 85.3 (d, 1C, C-3), 81.7 (d, 1C, C-4), 73.2, 71.4, 71.1 (t, 4C, O-CH2-Ph, C-6), 69.3 (d, 1C, C-2), 68.5 (t, 1C, C-9), 57.2 (t, 1C, C-5), 51.1 (t, 1C, C-7), 37.1 (q, 1C, Ms), 27.9 (t, 1C, C-8). **IR** ($CDCl_3$) ν = 3088, 3031, 2900, 2864, 2815, 1603, 1496, 1454, 1358, 1206, 1176, 1097 cm^{-1}. **MS-ESI** (m/z, %) = 561.00 (MNa^+, 67).

Synthesis of (2*R*,3*R*,4*R*)-1-(2-azidoethyl)-3,4-bis(benzyloxy)-2-[(benzyloxy)methyl] pyrrolidine (22), *Strategy a)*: A solution of mesylate **20** (40 mg, 0.076 mmol), 18-crown-6 ether (6.04 mg, 0.022 mmol) and sodium azide (9.89 mg, 0.15 mmol) in dry acetonitrile (1.5 mL) was stirred under nitrogen atmosphere at reflux for 3.5 h. The mixture was transferred to a separatory funnel and washed with H_2O. The aqueous layer was then extracted with CH_2Cl_2 (3 × 5 mL) and the combined organic layers were dried over Na_2SO_4. The solvent was evaporated under a vacuum and the crude was purified by FCC (CH_2Cl_2/Et_2O 100 : 1) affording pure **22** (9 mg, 0.019 mmol) with a 25% yield. $[\alpha]_D^{24} = -12.9$ (c = 0.34, $CHCl_3$). **^{1}H NMR** (400 MHz,$CDCl_3$) δ ppm = 7.28–7.18 (m, 15H, Ar), 4.49–4.34 (m, 6H, O-$\underline{CH_2}$-Ph), 3.88 (d, J = 4.4 Hz, 1H, H-4), 3.76 (d, J = 3.5 Hz, 1H, H-3), 3.48 (m, 2H, H-6), 3.31 (m, 1H, Ha-8), 3.21 (m, 2H, Hb-8, Ha-5) 3.09 (m, 1H, Ha-7), 2.77 (m, 1H, H-2), 2.59 (m, 2H, Hb-5, Hb-7). **^{13}C NMR** (50 MHz, $CDCl_3$) δ ppm = 138.4–138.2 (s, 3C, Ar), 128.6–127.6 (d, 15C, Ar), 85.2 (d, 1C, C-3), 81.8 (d, 1C, C-4), 73.3, 71.5, 71.1, (t, 4C, O-$\underline{CH_2}$-Ph, C-6), 69.4 (d, 1C, C-2), 57.5 (t, 1C, C-5), 54.3 (t, 1C, C-7), 49.9 (t, 1C, C-8). **IR** ($CDCl_3$) ν = 3066, 3032, 2926, 2857, 2103, 1602, 1496, 1454, 1365, 1271, 1206 cm^{-1}. **MS-ESI** (m/z, %) = 473.32 (MH^+, 100), 495.31 (MNa^+, 81.6).

Synthesis of (2*R*,3*R*,4*R*)-1-(2-azidoethyl)-3,4-bis(benzyloxy)-2-[(benzyloxy)methyl] pyrrolidine (22), *Strategy b)*: To a solution of alcohol **18** (83 mg, 0.18 mmol) in dry THF (2 mL) at 0 °C under nitrogen atmosphere, PPh_3 recrystallized from Et_2O (146 mg, 0.56 mmol) was added, followed by DIAD (109 µL, 0.56 mmol) and DPPA (133 µL, 0.59 mmol). The mixture was left to reach room temperature and maintained under nitrogen atmosphere for 2.5 h. The solvent was removed under reduced pressure and the crude purified by FCC (Et_2O:EtP 1:3), to yield compound **22** (77 mg, 0.16 mmol, 88%).

Synthesis of (2*R*,3*R*,4*R*)-1-(3-azidopropyl)-3,4-bis(benzyloxy)-2-[(benzyloxy)methyl] pyrrolidine (23): A solution of mesylate **21** (83 mg, 0.15 mmol), 18-crown-6 ether (8 mg, 0.03 mmol) and sodium azide (20 mg, 0.3 mmol) in dry acetonitrile (2.5 mL) was stirred under nitrogen atmosphere at reflux for 5 h. TLC analysis (EtP:AcOEt 1:1) showed the disappearance of the starting material (R_f = 0.49) and the formation of a new product (R_f = 0.86). The mixture was transferred to a separatory funnel and washed with H_2O. The aqueous layer was then extracted with CH_2Cl_2 (3 × 10 mL) and the combined organic layers were dried over Na_2SO_4. The solvent was evaporated under a vacuum and the crude was purified by FCC (CH_2Cl_2/Et_2O 25:1) affording pure **23** (70 mg, 0.14 mmol) with a 94% yield. $[\alpha]_D^{25} = -26.1$ (c = 0.64, $CHCl_3$). **^{1}H NMR** (400 MHz,$CDCl_3$) δ ppm = 7.36–7.25 (m, 15H, Ar), 4.56–4.43 (m, 6H, O-$\underline{CH_2}$-Ph), 3.94 (d, J = 4.9 Hz, 1H, H-4), 3.86 (d, J = 3.9 Hz, 1H, H-3), 3.59–3.51 (m, 2H, H-6), 3.32 (td, J = 6.5, 3.1 Hz, 2H, H-9), 3.18 (d, J = 10.7 Hz, 1H, Ha-5), 2.97 (dt, J = 12.2, 8.0 Hz, 1H, Ha-7), 2.75 (q, J = 5.2 Hz, 1H, H-2), 2.56 (dd, J = 10.5, 5.1 Hz, 1H, Hb-5), 2.42 (m, 1H, Hb-7), 1.45 (m, 2H, H-8). **^{13}C NMR** (50 MHz, $CDCl_3$) δ ppm = 138.4, 138.3 (s, 3C, Ar), 128.3, 127.5 (d, 15C, Ar), 85.5 (d, 1C, C-3), 81.9 (d, 1C, C-4), 73.3 (t, 1C, O-$\underline{CH_2}$-Ph), 71.4, 71.3 (t, 2C, O-$\underline{CH_2}$-Ph, C-6), 71.1 (t, 1C, O-$\underline{CH_2}$-Ph), 69.3 (d, 1C, C-2), 57.2 (t, 1C, C-5), 52.3 (t, 1C, C-7), 49.6 (t, 1C, C-9), 27.6 (t, 1C, C-8). **IR** ($CDCl_3$) ν = 3066, 3032, 2864, 2806, 2098, 1495, 1453, 1365, 1301, 1259, 1096, 1028 cm^{-1}. **MS-ESI** (m/z, %) = 509.20 (MNa^+, 100).

Synthesis of (4-{(2*R*,3*R*,4*R*)- 3,4-bis(benzyloxy)-2-[(benzyloxy) methyl] pyrrolidin-1yl}butyl)amine (24): [For an alternative synthesis of **24** see: [65] To a solution of azide **17** (74 mg, 0.15 mmol) in dry THF (2.5 mL) under nitrogen atmosphere PPh_3 (47 mg, 0.18 mmol) and

H_20 (5.36 μL, 0.30 mmol) were added. The mixture was heated at reflux overnight, then a TLC control (CH_2Cl_2:Et_2O 100:1 showed the disappearance of the starting material (R_f = 0.21). The mixture was diluted with H_2O, transferred to a separatory funnel and washed with H_2O. The aqueous layer was then extracted with CH_2Cl_2 (3 × 15 mL) and the combined organic layers were dried over Na_2SO_4. The solvent was evaporated under a vacuum and the crude was purified by FCC (AcOEt and then CH_2Cl_2: MeOH: NH_4OH 6% 4: 1: 0.1) affording pure **24** (59 mg, 0.12 mmol) with a 84% yield. $[\alpha]_D^{23} = -25.5$ (c = 0.595, $CHCl_3$). **^{1}H NMR** (400 MHz, $CDCl_3$) δ ppm = 7.34–7.25 (m, 15H, Ar), 4.56–4.42 (m, 6H, O-$\underline{CH_2}$-Ph), 3.91 (d, *J* = 4.9 Hz, 1H, H-4), 3.87 (d, *J* = 4.4 Hz, 1H, H-3), 3.55 (m, 2H, H-6), 3.21 (d, *J* = 10.2 Hz, 1H, Ha-5), 2.84 (m, 1H, Ha-7), 2.70 (m, 3H, H-2, H-10), 2.55 (dd, *J* = 10.2, 5.1 Hz, 1H, Hb-5), 2.34 (m, 1H, Hb-7), 1.55–1.41 (m, 4H, H-8, H-10). **^{13}C NMR** (50 MHz, $CDCl_3$) δ ppm = 138.5–138.4 (s, 3C, Ar), 128.3–127.5 (d, 15C, Ar), 85.6 (d, 1C, C-3), 81.8 (d, 1C, C-4), 73.2, 71.3, 71.1 (t, 4C, O-$\underline{CH_2}$-Ph, C-6), 69.3 (d, 1C, C-2), 57.2 (t, 1C, C-5), 55.3 (t, 1C, C-7), 42.0 (t, 1C, C-10), 31.6 (t, 1C, C-9), 25.6 (t, 1C, C-8). **IR** ($CDCl_3$) ν = 3320, 3306, 3090, 3066, 2931, 2863, 1601, 1495, 1454, 1366, 1095 cm^{-1}. **MS-ESI** (*m/z*, %) = 474.96 (MH^+, 100).

Synthesis of (2-{(2*R*,3*R*,4*R*)- 3,4-bis(benzyloxy)-2- [(benzyloxy) methyl] pyrrolidin-1yl}ethyl)amine (25): To a solution of azide **22** (77 mg, 0.16 mmol) in dry THF (2.5 mL) under nitrogen atmosphere PPh_3 (50 mg, 0.19 mmol) and H_20 (5.76 μL, 0.32 mmol) were added. The mixture was heated at reflux overnight, then a TLC control (CH_2Cl_2:Et_2O 100:1 showed the disappearance of the starting material (R_f = 0.36). The mixture was diluted with H_2O, transferred to a separatory funnel and washed with H_2O. The aqueous layer was then extracted with CH_2Cl_2 (3 × 15 mL) and the combined organic layers were dried over Na_2SO_4. The solvent was evaporated under a vacuum and the crude was purified by FCC (AcOEt and then CH_2Cl_2: MeOH 10: 1) affording pure **25** (45 mg, 0.10 mmol) with a 63% yield. $[\alpha]_D^{23} = -20.3$ (c = 0.785, $CHCl_3$). **^{1}H NMR** (400 MHz, $CDCl_3$) δ ppm = 7.34–7.20 (m, 15H, Ar), 4.50–4.39 (m, 6H, O-$\underline{CH_2}$-Ph), 3.94 (d, *J* = 4.8 Hz, 1H, H-4), 3.84 (d, *J* = 2.9 Hz, 1H, H-3), 3.52 (m, 2H, H-6), 3.19 (d, *J* = 10.3 Hz, 1H, Ha-5), 3.10 (dd, *J* = 10.5, 5.1 Hz, 1H, Hb-5), 2.99 (m, 1H, Ha-7), 2.79 (m, 3H, H-8, H-2), 2.53 (m, 1H, Hb-7), 1.96 (bs, 2H, NH_2). **^{13}C NMR** (50 MHz, $CDCl_3$) δ ppm = 138.1–138.0 (s, 3C, Ar), 128.4–127.6 (d, 15C, Ar), 85.0 (d, 1C, C-3), 81.8 (d, 1C, C-4), 73.2–71.5–71.2 (t, 3C, O-$\underline{CH_2}$-Ph), 70.3 (t, 1C, C-6), 69.1 (d, 1C, C-2), 57.3 (t, 1C, C-5), 54.6 (t, 1C, C-7), 38.9 (t, 1C, C-8). **IR** ($CDCl_3$) ν = 3378, 3032, 2925, 2863, 1595, 1495, 1454, 1366, 1207, 1094, 1076, 1028 cm^{-1}. **MS-ESI** (*m/z*, %) = 446.94 (MH^+, 100).

Synthesis of (3-{(2*R*,3*R*,4*R*)- 3,4-bis(benzyloxy)-2- [(benzyloxy) methyl] pyrrolidin-1yl}propyl)amine (26): To a solution of azide **22** (34 mg, 0.07 mmol) in MeOH (2 mL) under nitrogen atmosphere Pd/C (17 mg) was added, together with 3 drops of 37% aqueous HCl. The mixture was stirred under hydrogen atmosphere (balloon) for 18 h. The catalyst was filtered through Celite and the solvent evaporated under reduced pressure. The crude was purified on DOWEX-50WX8 resin, eluting sequentially with MeOH (10 mL), H_2O (10 mL) and 6% NH_4OH. The free amine **26** (11 mg, 0.058 mmol) was recovered with a 86% yield. $[\alpha]_D^{21} = -40.3$ (c = 0.845, CH_3OH). **^{1}H NMR** (400 MHz, CD_3OD) δ ppm = 3.94 (d, *J* = 5.1 Hz, 1H, H-4), 3.87 (dd, *J* = 4.3, 1.9 Hz, 1H, H-3), 3.68 (m, 2H, H-6), 3.05 (d, *J* = 10.4 Hz, 1H, Ha-5), 2.94 (dt, *J* = 12.0, 8.0 Hz, 1H, Ha-7), 2.81 (t, *J* = 6.5 Hz, 1H, Ha-9), 2.79 (t, *J* = 6.5 Hz, 1H, Hb-9), 2.61 (dd, *J* = 10.4, 5.1 Hz, 1H, Hb-5), 2.41 (m, 2H, Hb-7, H-2), 1.69 (m, 2H, H-8). **^{13}C NMR** (50 MHz, CD_3OD) δ ppm = 79.3 (d, 1C, C-3), 75.9 (d, 1C, C-4), 72.7 (d, 1C, C-2), 60.6 (t, 1C, C-6), 58.9 (t, 1C, C-5), 52.6 (t, 1C, C-7), 39.7 (t, 1C, C-9), 27.8 (t, 1C, C-8). **MS-ESI** (*m/z*, %) = 190.85 (MH^+, 100).

Synthesis of 1-(2-{(2*R*,3*R*,4*R*)-3,4-bis(benzyloxy)-2- [(benzyloxy)methyl] pyrrolidin-1-yl}ethyl)-4-(4-nitrophenyl)-1-*H*-1,2,3-triazole (27): To a solution of azide **22** (72 mg, 0.15 mmol) in THF (1.5 mL), a catalytic amount (2.86 mg, 0.015 mmol) of CuI, 1-ethynyl-4-nitrobenzene(26.5 mg, 0.18 mmol) and DIPEA (DIPEA, 31 μL, 0.18 mmol) were added: The solution was stirred at room temperature for 2 h, when a TLC analysis (Et_2O/PE 1:3) attested the disappearance of the starting material **22** (R_f = 0.22) and the formation of a new product (R_f = 0.03). The reaction mixture was concentrated under a vacuum and the resulting crude was purified by FCC (PE/AcOEt 2:1), affording 47 mg (0.08 mmol) of pure **27**, with a 53% yield. $[\alpha]_D^{25} = +20.5$ (c = 0.185, $CHCl_3$). **^{1}H NMR** (400 MHz, $CDCl_3$) δ ppm = 8.04 (m, 2H, Ar *o*-NO_2), 8.03 (s, 1H, triazole), 7.67 (m, 2H, Ar *m*-NO_2), 7.27–7.09 (m, 15H, Ar), 4.52–4.30 (m, 8H, O-$\underline{CH_2}$-Ph, H-8), 3.91 (d, *J* = 4.9 Hz, 1H, H-4), 3.77 (d, *J* = 3.9 Hz, 1H, H-3), 3.41 (m, 1H, Ha-6), 3.34–3.24 (m, 2H, Hb-6, Ha-7), 3.12 (d, *J* = 10.2 Hz, 1H, Ha-5), 2.89–2.79 (m, 2H, H-2, Hb-7), 2.68 (dd, *J* = 10.2, 4.9 Hz, 1H, Hb-5). **^{13}C NMR** (50 MHz, $CDCl_3$) δ ppm = 147.1 (s, 1C, $\underline{C}$-NO_2), 145.1, 137.9, 137.2 (s, 5C, Ar *p*-NO_2, Ar, triazole), 128.4–127.6 (d, 15C, Ar), 125.8 (d, 2C, Ar *m*-NO_2), 124.1 (d, 2C, Ar *o*-NO_2), 122.7 (d, 1C, triazole), 85.0 (d, 1C, C-3), 81.9 (d, 1C, C-4), 73.3 (t, 1C, O-$\underline{CH_2}$-Ph), 71.6 (t, 1C, C-6), 71.3 (t, 2C, O-$\underline{CH_2}$-Ph), 69.2 (d, 1C, C-2), 57.3 (t, 1C, C-5), 53.7 (t, 1C, C-7), 49.1 (t, 1C, C-8). **IR** ($CDCl_3$) ν = 3066, 3030, 2860, 2602, 1518, 1453, 1347, 1234, 1109 cm^{-1}. **MS-ESI** (*m/z*, %) = 619.95 (MH^+, 31), 642.05 (MNa^+, 100).

Synthesis of 1-(3-{(2*R*,3*R*,4*R*)-3,4-bis(benzyloxy)-2- [(benzyloxy)methyl] pyrrolidin-1-yl}propyl)-4-(4-nitrophenyl)-1*H*-1,2,3-triazole (28): Azide **23** (32 mg, 0.066 mmol) was dissolved in a 2:1 THF/H_2O mixture (2.7 mL total volume) in a MW vial reactor and $CuSO_4$ (3.1 mg, 0.021 mmol), sodium ascorbate (8.3 mg, 0.042 mmol) and 1-ethynyl-4-nitrobenzene (11.6 mg, 0.083 mmol) were added. The reaction mixture was heated in the MW at 80 °C for 45 min, when a TLC analysis (eluent CH_2Cl_2/Et_2O 30: 1) attested the disappearance of the starting material **23** (R_f = 0.46) and the formation of a new product (R_f = 0.17). The reaction mixture was filtered over Celite and concentrated under reduced pressure. The resulting crude product was purified by FCC (PE/AcOet 1:1) affording 36 mg (0.057 mmol) of compound **28** with a 87% yield. $[\alpha]_D^{25} = -14.2$ (c = 0.9, $CHCl_3$). **^{1}H NMR** (400 MHz, $CDCl_3$) δ ppm = 8.12 (m, 2H, Ar *o*-NO_2), 7.89 (s, 1H, triazole), 7.81 (m, 2H, Ar *p*-NO_2), 7.27–7.15 (m, 15H, Ar), 4.46–4.33 (m, 8H, O-$\underline{CH_2}$-Ph, H-9), 3.88 (d, *J* = 5.8 Hz, 1H, H-4), 3.79 (d, *J* = 4.3 Hz, 1H, H-3), 3.51–3.44 (m, 2H, H-6), 3.05 (d, *J* = 10.3 Hz, 1H, Ha-5), 2.88–2.81 (m, 1H, Ha-7), 2.65 (q, *J* = 5.0 Hz, 1H, H-2), 2.48 (dd, *J* = 10.3, 5.4 Hz, 1H, Hb-5), 2.38–2.32 (ddd, *J* = 4.9, 6.3, 11.2 Hz, 1H, Hb-7), 2.08–2.00 (m, 2H, H-8). **^{13}C NMR** (50 MHz, $CDCl_3$) δ ppm = 147.2 (s, 1C, $\underline{C}$-NO_2), 145.2, 138.1, 137.1 (s, 5C, Ar *p*-NO_2, Ar, triazole), 128.3–127.6 (d, 15C, Ar), 126.0 (d, 2C, Ar *m*-NO_2), 124.1 (d, 2C, Ar *o*-NO_2), 122.1 (d, 1C, triazole), 85.2 (d, 1C, C-3), 81.8 (d, 1C, C-4), 73.3–71.2 (t, 3C, O-$\underline{CH_2}$-Ph), 70.9 (t, 1C, C-6), 69.3 (t, 1C, C-2), 57.3 (t, 1C, C-5), 51.8 (t, 1C, C-7), 48.5 (t, 1C, C-9), 28.6 (t, 1C, C-8). **IR** ($CDCl_3$) ν = 3066, 3031, 2926, 2858, 1607, 1521, 1454, 1344, 1232, 1205, 1110, 1075 cm^{-1}. **MS-ESI** (*m/z*, %) = 656.31 (MNa^+, 100).

Synthesis of 1-(4-{(2*R*,3*R*,4*R*)-3,4-bis(benzyloxy)-2- [(benzyloxy)methyl] pyrrolidin-1-yl}butyl)-4-(4-nitrophenyl)-1*H*-1,2,3-triazole (29): Azide **17** (21 mg, 0.042 mmol) was dissolved in a 2:1 THF/H_2O mixture (1.50 mL total volume) in a MW vial reactor and $CuSO_4$ (2.0 mg, 0.012 mmol), sodium ascorbate (5.0 mg, 0.025 mmol) and 1-ethynyl-4-nitrobenzene (7.4 mg, 0.05 mmol) were added. The reaction mixture was heated in the MW at 80 °C for 45 min, when a TLC analysis (eluent CH_2Cl_2/Et_2O 50: 1) attested the disappearance of the starting material **23** ((R_f = 0.51) and the formation of a new product (R_f = 0.28). The reaction mixture was filtered over Celite and concentrated under reduced pressure. The resulting crude product was purified by FCC (PE/AcOet 1:1) affording 25 mg (0.039 mmol) of compound **29** with a 92% yield. $[\alpha]_D^{25} = -13.9$ (c = 0.15, $CHCl_3$). **^{1}H NMR** (400 MHz, $CDCl_3$) δ ppm = 8.17 (m, 2H, Ar *o*-NO_2), 7.86 (m, 2H, Ar *m*-NO_2), 7.75 (s, 1H, triazole), 7.26–7.16 (m, 15H, Ar), 4.43–4.30 (m, 8H, O-$\underline{CH_2}$-Ph, H-10), 3.86 (d, *J* = 5.3 Hz, 1H, H-4), 3.78 (d, *J* = 3.9 Hz, 1H, H-3), 3.49 (m, 2H, H-6), 3.09 (d, *J* = 10.7 Hz, 1H, Ha-5), 2.86 (m, 1H, Ha-7), 2.65 (q, *J* = 5.0 Hz, 1H, H-2), 2.45 (dd, *J* = 10.5, 5.1 Hz, 1H, Hb-5), 2.33 (m, 1H, Hb-7), 1.92 (m, 2H, H-9),

1.45 (m, 2H, H-8). **^{13}C NMR** (50 MHz, $CDCl_3$) δ ppm = 147.3 (s, 1C, C-NO_2), 145.4, 138.3, 138.1, 138.2, 137.1 (s, 5C, Ar *p*-NO_2, Ar, triazole), 128.3, 127.7 (d, 15C, Ar), 126.1 (d, 2C, Ar *m*-NO_2), 124.2 (d, 2C, Ar *o*-NO_2), 121.1 (d, 1C, triazole), 85.3 (d, 1C, C-3), 81.8 (d, 1C, C-4), 73.2 (t, 1C, O-CH_2-Ph), 71.5–71.3 (d, 2C, C-6, O-CH_2-Ph), 71.1 (t, 1C, O-CH_2-Ph), 69.3 (d, 1C, C-2), 57.3 (t, 1C, C-5), 54.3 (t, 1C, C-7), 50.1 (t, 1C, C-10), 28.2 (t, 1C, C-9), 24.7 (t, 1C, C-8). **IR** ($CDCl_3$) ν = 3087, 3032, 2928, 2862, 1606, 1497, 1454, 1230, 1207, 1109 cm^{-1}. **MS-ESI** (*m/z*, %) = 670.36 (MNa^+, 100), 648.35 (MH^+, 14).

Synthesis of (2*R*,3*R*,4*R*)-2-(hydroxymethyl)-1-{2-[4-(4-nitrophenyl)-1*H*-1,2,3-triazol-1-yl] ethyl}pyrrolidine-3,4-diol (9): A solution of compound **27** (35 mg, 0.056 mmol) in dry CH_2Cl_2 (5.6 mL) was cooled at 0 °C (ice bath) under nitrogen atmosphere and a 1 M solution of BCl_3 in hexane (0.51 mL) was added. The reaction mixture was left to reach room temperature and stirred for 18 h, when a TLC analysis (eluent PE/AcOEt 1:1) attested the disappearance of the starting material **27** (R_f = 0.5). EtOH was added until a homogeneous mixture was obtained, then the solvents were evaporated under a vacuum. The resulting solid was solved in the minimum amount of H_2O and the basic resin Ambersep 900-OH was added. The suspension was stirred for 40 min and filtered on cotton, extensively washing with MeOH. The mixture was concentrated under reduced pressure and the crude was purified by FCC (CH_2Cl_2/MeOH 5:1) to obtain pure **9** (12.3 mg, 0.035 mmol) with a 63% yield. **$[\alpha]_D^{22}$** = −6.2 (c = 0.21, CH_3OH). **^{1}H NMR** (400 MHz, D_2O) δ ppm = 8.32 (s, 1H, triazole), 8.05 (m, 2H, Ar *o*-NO_2), 7.70 (m, 2H, Ar *m*-NO_2), 4.45 (t, *J* = 6.1 Hz, 2H, H-8), 3.98 (m, 1H, H-4), 3.77 (m, 1H, H-3), 3.48 (m, 2H, H-6), 3.25 (m, 1H, Ha-7), 2.85 (m, 2H, Hb-7, Ha-5), 2.67 (m, 1H, Hb-5), 2.48 (q, *J* = 4.9 Hz, 1H, H-2). **^{13}C NMR** (50 MHz, D_2O) δ ppm = 147.2, 145.6, 136.2 (s, 3C, C-NO_2, Ar *p*-NO_2, triazole), 126.3 (d, 2C, Ar *m*-NO_2), 124.5 (d, 2C, Ar *o*-NO_2), 124.1 (d, 1C, triazole), 78.9 (d, 1C, C-3), 75.7 (d, 1C, C-4), 71.7 (d, 1C, C-2), 61.0 (t, 1C, C-6), 58.4 (t, 1C, C-5), 53.8 (t, 1C, C-7), 49.2 (t, 1C, C-8). **MS-ESI** (*m/z*, %) = 372.12 (MNa^+, 100).

Synthesis of (2*R*,3*R*,4*R*)-2-(hydroxymethyl)-1-{3-[4-(4-nitrophenyl)-1*H*-1,2,3-triazol-1-yl] propyl} pyrrolidine-3,4-diol (10): A solution of compound **28** (50 mg, 0.079 mmol) in dry CH_2Cl_2 (7.9 mL) was cooled at 0 °C (ice bath) under nitrogen atmosphere and a 1 M solution of BCl_3 in hexane (0.71 mL) was added. The reaction mixture was left to reach room temperature and stirred for 18 h, when a TLC analysis (eluent PE/AcOEt 1:2) attested the disappearance of the starting material **28** (R_f = 0.65). EtOH was added until a homogeneous mixture was obtained, then the solvents were evaporated under a vacuum. The resulting solid was dissolved in the minimum amount of H_2O and the basic resin Ambersep 900-OH was added. The suspension was stirred for 30 min and filtered on cotton, extensively washing with MeOH. The mixture was concentrated under reduced pressure and the crude was purified by FCC (CH_2Cl_2/MeOH 9:1) to obtain pure **10** (21.2 mg, 0.058 mmol) with a 74% yield. **$[\alpha]_D^{24}$** = −34.7 (c = 0.80, CH_3OH). **^{1}H NMR** (400 MHz, CD_3OD) δ ppm = 8.61 (s, 1H, triazole), 8.29 (m, 2H, Ar *o*-NO_2), 8.06 (m, 2H, Ar *m*-NO_2), 4.58 (m, 2H, H-9), 3.94 (m, 2H, H-3, H-4), 3.64 (m, 2H, H-6), 3.06 (d, *J* = 10.3 Hz, 1H, Ha-5), 2.83 (dt, *J* = 12.2, 8.1 Hz, 1H, Ha-7), 2.63 (dd, *J* = 10.2, 5.1 Hz, 1H, Hb-5), 2.39 (m, 2H, Hb-7, H-2), 2.13 (m, 2H, H-8). **^{13}C NMR** (50 MHz, CD_3OD) δ ppm = 147.3, 145.2, 136.9 (s, 3C, C-NO_2, Ar *p*-NO2, triazole), 125.8 (d, 2C, Ar *m*-NO_2), 123.8 (d, 2C, Ar *o*-NO_2), 123.0 (d, 1C, triazole), 79.4 (d, 1C, C-3), 75.9 (d, 1C, C-4), 73.0 (d, 1C, C-2), 60.9 (t, 1C, C-6), 58.7 (t, 1C, C-5), 51.0 (t, 1C, C-7), 47.9 (t, 1C, C-9), 28.3 (t, 1C, C-8). **MS-ESI** (*m/z*, %) = 394.21 (MH^+,100). **HRESI-MS** *m/z* found 364.1616, calc. for $C_{16}H_{22}N_5O_5^+$ [MH^+]: 364.1612.

Synthesis of (2*R*,3*R*,4*R*)-2-(hydroxymethyl)-1-{4-[4-(4-nitrophenyl)-1*H*-1,2,3-triazol-1-yl] butyl}pyrrolidine-3,4-diol (11): A solution of compound **29** (22 mg, 0.034 mmol) in dry CH_2Cl_2 (3.4 mL) was cooled at 0 °C (ice bath) under nitrogen atmosphere and a 1 M solution of BCl_3 in hexane (0.71 mL) was added. The reaction mixture was left to reach room temperature and stirred for 18 h, when a TLC analysis (eluent PE/AcOEt 1:2) attested the disappearance of the starting material **29** (R_f = 0.65). EtOH was added until a homogeneous mixture was obtained, then the solvents were evaporated under a vacuum. The resulting solid was dissolved in the minimum amount of H_2O and the basic resin Ambersep 900-OH was added. The suspension was stirred for 30 min and filtered on cotton, extensively washing with MeOH. The mixture was concentrated under reduced pressure and the crude was purified by FCC (CH_2Cl_2/MeOH 7:1) to obtain pure **11** (10.3 mg, 0.027 mmol) with a 80% yield. **$[\alpha]_D^{25}$** = −25.2 (c = 0.44, CH_3OH). **^{1}H NMR** (400 MHz, CD_3OD) δ ppm = 8.58 (s, 1H, triazole), 8.31 (m, 2H, Ar *o*-NO_2), 8.07 (m, 2H, Ar *m*-NO_2), 4.52 (t, *J* = 7.0 Hz, 2H, H-10), 3.94 (d, *J* = 5.2 Hz, 1H, H-4), 3.89 (m, 1H, H-3), 3.67 (m, 2H, H-6), 3.02 (d, *J* = 10.3 Hz, 1H, Ha-5), 2.94 (m, 1H, Ha-7), 2.66 (dd, *J* = 10.3, 5.2 Hz, 1H, Hb-5), 2.45 (m, 2H, Hb-7, H-2), 2.01 (m, 2H, H-9), 1.56 (q, *J* = 7.4 Hz, 2H, H-8). **^{13}C NMR** (50 MHz, CD_3OD) δ ppm = 147.3 (s, 1C, C-NO_2), 145.3, 136.9 (s, 2C, Ar *p*-NO_2, triazole), 125.9 (d, 2C, Ar *m*-NO_2), 123.8 (d, 2C, *o*-NO_2), 122.6 (d, 1C, triazole), 79.3 (d, 1C, C-3), 75.8 (d, 1C, C-4), 73.3 (d, 1C, C-2), 61.1 (t, 1C, C-6), 59.0 (t, 1C, C-5), 54.2 (t, 1C, C-7), 49.9 (t, 1C, C-10), 27.6 (t, 1C, C-9), 24.4 (t, 1C, C-8). **MS-ESI** (*m/z*, %) = 400.22 (MNa^+, 100). **HRESI-MS** *m/z* found 378.1767, calc. for $C_{17}H_{24}N_5O_5^+$ [MH^+]: 378.1772.

Synthesis of *N*-{3-[(2*R*,3*R*,4*R*)-3,4-dihydroxy-2-(hydroxymethyl) pyrrolidin-1-yl] propyl}-4-nitrobenzamide (13): Amine **26** (32 mg, 0.17 mmol) was solved in dry pyridine (2 mL) and 4-nitrobenzoyl chloride (31 mg, 0.17 mmol) was added. The reaction mixture was stirred at room temperature for 22 h. Then, the pyridine was evaporated under vacuum and the resulting crude was purified by FCC (CH_2Cl_2/MeOH/6% NH_4OH 5:1:0.1), leading to compound **13** (28 mg, 0.083 mmol) with a 49% yield. **$[\alpha]_D^{25}$** = −13.2 (c = 0.82, CH_3OH). **^{1}H NMR** (400 MHz, CD_3OD) δ ppm = 8.30 (m, 2H, Ar *o*-NO_2), 8.05 (m, 2H, Ar *m*-NO_2), 3.98 (m, 1H, H-4), 3.92 (m, 1H, H-3), 3.69 (m, 2H, H-6), 3.62–3.37 (m, 2H, H-9), 3.09 (m, 2H, Ha-7, Ha-5), 2.70 (dd, *J* = 10.3, 4.1 Hz, 1H, Hb-5), 2.52 (m, 2H, Hb-7, H-2), 1.83 (m, 2H, H-8). **^{13}C NMR** (50 MHz, CD_3OD) δ ppm = 166.1 (s, 1C, C═O), 149.6, 140.0 (s, 2C, C-NO_2, Ar *p*-NO_2), 128.3 (d, 2C, Ar *m*-NO_2), 123.1 (d, 2C, Ar *o*-NO_2), 79.1 (d, 1C, C-3), 75.8 (d, 1C, C-4), 73.5 (d, 1C, C-2), 60.8 (t, 1C, C-6), 59.1 (t, 1C, C-7), 53.2 (t, 1C, C-5), 38.6 (t, 1C, C-9), 26.7 (t, 1C, C-8). **MS-ESI** (*m/z*, %) = 340.12 (MH^+, 100). **HRESI-MS** *m/z* found 340.1495, calc. for $C_{15}H_{22}N_3O_6^+$ [MH^+]: 340.1503.

Synthesis of *N*-(2-{(2*R*,3*R*,4*R*)-3,4-bis(benzyloxy)-2-[(benzyloxy)methyl] pyrrolidin-1-yl}ethyl)-4-nitrobenzamide (34): Amine **25** (28 mg, 0.063 mmol) was dissolved in dry pyridine (1.5 mL) and 4-nitrobenzoyl chloride (17 mg, 0.092 mmol) was added. The reaction mixture was stirred at room temperature for 28 h, when a TLC analysis attested the disappearance of the starting material **25**. The pyridine was evaporated under a vacuum and the resulting crude was purified by FCC (CH_2Cl_2/MeOH 50:1), leading to compound **34** (21 mg, 0.035 mmol) with a 56% yield. **$[\alpha]_D^{23}$** = −15.8 (c = 1.175, $CHCl_3$). **^{1}H NMR** (400 MHz, $CDCl_3$) δ ppm = 7.87 (m, 2H, Ar *o*-NO_2), 7.67 (m, 2H, Ar *m*-NO_2), 7.20 (m, 15H, Ar), 4.43 (m, 6H, O-CH_2-Ph), 3.67 (d, *J* = 5.4 Hz, 1H, H-4), 3.86 (d, *J* = 3.9 Hz, 1H, H-3), 3.56 (m, 3H, H-6, Ha-8), 3.29 (m, 1H, Hb-8), 3.18 (d, *J* = 10.2 Hz, 1H, Ha-5), 3.02 (m, 1H, Ha-7), 2.79 (m, 1H, H-2), 2.63 (m, 2H, Hb-5, Hb-7). **^{13}C NMR** (50 MHz, $CDCl_3$) δ ppm = 165.1 (s, 1C, C═O), 149.3 (s, 1C, C-NO_2), 140.0 (s, 1C, Ar *p*-NO_2), 137.9, 137.8 (s, 3C, Ar), 128.4, 127.5 (d, 17C, Ar, Ar *m*-NO_2), 123.5 (d, 2C, Ar *o*-NO_2), 84.8 (d, 1C, C-3), 81.6 (d, 1C, C-4), 73.4, 71.7, 71.3 (t, 3C, O-CH_2-Ph), 70.2 (t, 1C, C-6), 68.6 (d, 1C, C-2), 56.8 (t, 1C, C-5), 51.9 (t, 1C, C-7), 38.0 (t, 1C, C-8). **IR** ($CDCl_3$) ν = 3357, 3088, 3067, 3032, 2960, 2863, 1659, 1601, 1526, 1496, 1485, 1454, 1348, 1261 cm^{-1}. **MS-ESI** (*m/z*, %) = 618.37 (MNa^+, 100).

Synthesis of *N*-(4-{(2*R*,3*R*,4*R*)-3,4-bis(benzyloxy)-2-[(benzyloxy)methyl] pyrrolidin-1-yl}butyl)-4-nitrobenzamide (35): Amine **24** (37 mg, 0.078 mmol) was dissolved in dry pyridine (2 mL) and 4-nitrobenzoyl chloride (19 mg, 0.10 mmol) was added. The reaction mixture was stirred at room temperature for 40 h, when a TLC analysis (eluent CH_2Cl_2/MeOH/6% NH_4OH 4:1:0.1) attested the disappearance

of the starting material **24** (R_f = 0.54). The pyridine was evaporated under a vacuum and the resulting crude was purified by FCC (CH_2Cl_2/MeOH 30:1), leading to compound **35** (30 mg, 0.048 mmol) with a 62% yield. $[\alpha]_D^{23}$ = −2.3 (c = 1.05, $CHCl_3$). **^{1}H NMR** (400 MHz, $CDCl_3$) δ ppm = 8.00 (m, 2H, Ar *o*-NO_2), 7.78 (m, 2H, Ar *m*-NO_2), 7.29–7.11 (m, 15H, Ar), 4.47–4.26 (m, 6H, O-$\underline{CH_2}$-Ph), 3.86 (d, *J* = 5.3 Hz, 1H, H-4), 3.80 (d, *J* = 4.9 Hz, 1H, H-3), 3.50–3.32 (m, 4H, H-6, H-10), 5.13 (d, *J* = 10.7 Hz, 1H, Ha-5), 2.85–2.79 (m, 1H, Ha-7), 2.54 (q, *J* = 5.0 Hz, 1H, H-2), 2.42 (dd, *J* = 10.7, 5.3 Hz, 1H, Hb-5), 2.26 (m, 1H, Hb-7), 1.68 (m, 1H, Ha-9), 1.55 (m, 3H, H-8, Hb-9). **^{13}C NMR** (50 MHz, $CDCl_3$) δ ppm = 165.5 (s, 1C, C═O), 149.3 (s, 1C, C-NO_2), 140.4 (s, 1C, Ar *p*-NO_2), 137.9–137.7 (s, 3C, Ar), 128.4–127.7 (d, 17C, Ar, Ar *m*-NO_2), 123.4 (d, 2C, Ar *o*-NO_2), 84.9 (d, 1C, C-3), 81.4 (d, 1C, C-4), 73.2, 71.6, 71.3 (t, 3C, O-$\underline{CH_2}$-Ph), 70.1 (d, 1C, C-2), 69.7 (t, 1C, C-6), 57.5 (t, 1C, C-5), 54.8 (t, 1C, C-7), 39.6 (t, 1C, C-10), 27.3 (t, 1C, C-9), 25.3 (t, 1C, C-8). **IR** ($CDCl_3$) ν = 3449, 3282, 3088, 2930, 2863, 2811, 1662, 1601, 1526, 1454, 1348, 1318, 1298, 1262, 1098 cm^{-1}. **MS-ESI** (*m/z*, %) = 624.28 (MH^+, 63), 646.30 (MNa^+, 100).

Synthesis of *N*-{2-[(2*R*,3*R*,4*R*)-3,4-dihydroxy-2-(hydroxymethyl)pyrrolidin-1-yl] ethyl}-4-nitrobenzamide (12): A solution of compound **34** (21 mg, 0.035 mmol) in dry CH_2Cl_2 (3.5 mL) was cooled to 0 °C (ice bath) under nitrogen atmosphere and a 1 M solution of BCl_3 in hexane (0.32 mL) was added. The reaction mixture was left to reach room temperature and stirred for 15 h, when a **^{1}H** NMR control attested the disappearance of the starting material **34** (disappearance of multiplet at δ = 7.26 ppm, relative to benzylic protons). EtOH was added until a homogeneous mixture was obtained, then the solvents were evaporated under a vacuum. The resulting crude was passed through an ion exchange resin DOWEX-50WX8, eluting with MeOH, H_2O and 6% NH_4OH, and subsequently purified via FCC (CH_2Cl_2/MeOH 5:1) affording pure **12** (8.0 mg, 0.025 mmol) with a 70% yield. $[\alpha]_D^{23}$ = −18.9 (c = 0.55, CH_3OH). **^{1}H NMR** (400 MHz, CD_3OD) δ ppm = 8.31 (m, 2H, Ar *o*-NO_2), 8.04 (m, 2H, Ar *m*-NO_2), 4.00 (m, 1H, H-4), 3.91 (m, 1H, H-3), 3.74–3.61 (m, 3H, H-6, Ha-8), 3.46 (m, 1H, Hb-8), 3.16 (m, 2H, Ha-5, Ha-7), 2.83 (m, 1H, Hb-5), 2.71 (m, 1H, Hb-7), 2.61 (m, 1H, H-2). **^{13}C NMR** (100 MHz, CD_3OD) δ ppm = 166.9 (s, 1C, C═O), 149.6 (s, 1C, $\underline{C}$-NO_2), 139.9 (s, 1C, Ar *p*-NO_2), 128.3 (d, 2C, Ar *m*-NO_2), 123.2 (d, 2C, Ar *o*-NO_2), 78.9 (d, 1C, C-3), 75.8 (d, 1C, C-4), 73.4 (d, 1C, C-2), 60.8 (t, 1C, C-6), 60.0 (t, 1C, C-5), 53.7 (t, 1C, C-7), 38.3 (t, 1C, C-8). **MS-ESI** (*m/z*, %) = 348.16 (MNa^+, 100). **HRESI-MS** *m/z* found 326.1345, calc. for $C_{14}H_{20}N_3O_6^+$ [MH^+]: 326.1347.

Synthesis of *N*-{4-[(2*R*,3*R*,4*R*)-3,4-dihydroxy-2-(hydroxymethyl)pyrrolidin-1-yl] butyl}-4-nitrobenzamide (14): A solution of compound **35** (25 mg, 0.040 mmol) in dry CH_2Cl_2 (4 mL) was cooled to 0 °C (ice bath) under nitrogen atmosphere and a 1 M solution of BCl_3 in hexane (0.36 mL) was added. The reaction mixture was left to reach room temperature and stirred for 15 h, when a **^{1}H** NMR control attested the disappearance of the starting material **34** (disappearance of multiplet at δ = 7.26 ppm, relative to benzylic protons). EtOH was added until a homogeneous mixture was obtained, then the solvents were evaporated under a vacuum. The resulting crude was purified via FCC (CH_2Cl_2/MeOH/ 6% NH_4OH 5: 1:0.1) affording pure **14** (12.0 mg, 0.034 mmol) with a 85% yield. $[\alpha]_D^{26}$ = −21.3 (c = 0.53, CH_3OH). **^{1}H NMR** (400 MHz, CD_3OD) δ ppm = 8.31 (m, 2H, Ar *o*-NO_2), 8.01 (m, 2H, Ar *m*-NO_2), 3.98 (m, 1H, H-4), 3.90 (m, 1H, H-3), 3.71 (m, 2H, H-6), 3.41 (t, *J* = 6.6 Hz, 2H, H-10), 3.12 (d, *J* = 10.5 Hz, 1H, Ha-5), 3.02 (m, 1H, Ha-7), 2.79 (dd, *J* = 10.5 Hz, 4.9 Hz, 1H, Hb-5), 2.60 (m, 2H, Hb-7, H-2), 1.66 (m, 4H, H-8, H-9). **^{13}C NMR** (50 MHz, CD_3OD) δ ppm = 166.8 (s, 1C, C═O), 149.6 (s, 1C, $\underline{C}$-NO_2), 140.2 (s, 1C, Ar *p*-NO_2), 128.2 (d, 2C, Ar *m*-NO_2), 123.2 (d, 2C, Ar *o*-NO_2), 79.0 (d, 1C, C-3), 75.7 (d, 1C, C-4), 73.7 (d, 1C, C-2), 60.8 (t, 1C, C-6), 59.1 (t, 1C, C-5), 54.9 (t, 1C, C-7), 39.4 (t, 1C, C-10), 26.7, 24.6 (t, 2C, C-8, C-9). **MS-ESI** (*m/z*, %) = 354.19 (MH^+, 53), 376.24 (MNa^+, 100). **HRESI-MS** *m/z* found 354.1664, calc. for $C_{16}H_{24}N_3O_6^+$ [MH^+]: 354.1660.

Synthesis of the trivalent iminosugar 37: Azide **22** (106 mg, 0.22 mmol) and trivalent scaffold **36** (14 mg, 0.059 mmol)were dissolved in a 2:1 THF/H_2O mixture (7.5 mL total volume) in a MW vial reactor and $CuSO_4$ (9 mg, 0.06 mmol), sodium ascorbate (24 mg, 0.12 mmol) and 1-ethynyl-4-nitrobenzene (11.6 mg, 0.083 mmol) were added. The reaction mixture was heated in the MW at 80 °C for 45 min, when a TLC analysis (eluent AcOEt) attested the disappearance of the scaffold **36** (R_f = 0.47). The reaction mixture was filtered over Celite and concentrated under reduced pressure. The resulting crude product was purified by FCC (CH_2Cl_2/MeOH 20:1) and subsequent size exclusion chromatography with Sephadex, affording 67 mg (0.04 mmol) of compound **37** with a 68% yield. $[\alpha]_D^{24}$ = −14.6 (c = 1.34, $CHCl_3$). **^{1}H NMR** (400 MHz, $CDCl_3$) δ ppm = 7.58 (s, 3H, triazole), 7.34–7.24 (m, 45H, Ar), 4.49–4.33 (m, 30H, H-8, H-9, O-$\underline{CH_2}$-Ph), 3.94 (m, 3H, H-4), 3.80 (m, 3H, H-3), 3.47 (m, 6H, H-6), 3.34 (m, 9H, H-10, Ha-7), 3.19 (d, *J* = 10.4 Hz, 3H, Ha-5), 2.86 (m, 6H, H-2, Hb-7), 2.68 (dd, *J* = 10.2, 5.1 Hz, 3H, Hb-5). **^{13}C NMR** (50 MHz, $CDCl_3$) δ ppm = 144.6 (s, 3C, triazole), 138.1, 138.0 (s, 9C, Ar), 128.4, 128.3, 127.7 (d, 45C, Ar), 123.4 (d, 3C, triazole), 85.1 (d, 3C, C-3), 81.6 (d, 3C, C-4), 73.2 (t, 3C, O-$\underline{CH_2}$-Ph), 72.1 (s, 1C, *scaffold*), 71.5, 71.3, 71.1 (t, 12C, O-$\underline{CH_2}$-Ph, C-6, C-10), 69.1 (d, 3C, C-2), 64.8 (t, 3C, C-9), 57.3 (t, 3C, C-5), 54.4 (t, 3C, C-7), 48.9 (t, 3C, C-8). **IR** ($CDCl_3$) ν = 3377, 3089, 3066, 3032, 2924, 2864, 1722, 1496, 1454, 1363, 1263, 1206, 1097, 1054 cm^{-1}. **MS-ESI** (*m/z*, %) = 1674.58 (MNa^+, 92).

Synthesis of trivalent iminosugar bearing the 4-nitrobenzene moiety 38: Trivalent iminosugar **37** (67 mg, 0.04 mmol) was dissolved in dry CH_2Cl_2 (4 mL) and DIPEA (20 μL, 0.12 mmol) was added, under nitrogen atmosphere. The reaction mixture was cooled at 0 °C (ice bath) and 4-nitrobenzoyl chloride (9 mg, 0.049 mmol) was added. The reaction mixture was stirred at room temperature for 2 days, when a TLC analysis (eluent CH_2Cl_2/MeOH 30:1) attested the disappearance of the starting material **37** (R_f = 0.22) and the formation of a new product (R_f = 0.34). The reaction was transferred to a separatory funnel and washed with 0.5 M HCl (2 × 5 mL) and H_2O (3 × 10 mL). The combined organic layers were dried over Na_2SO_4 and the solvent was removed under a vacuum. The resulting crude was purified by FCC (CH_2Cl_2/MeOH 30:1), leading to compound **38** (61 mg, 0.034 mmol) with a 85% yield. $[\alpha]_D^{25}$ = −18.7 (c = 0.92, $CHCl_3$). **^{1}H NMR** (400 MHz, $CDCl_3$) δ ppm = 8.12 (m, 2H, Ar *o*-NO_2), 7.95 (m, 2H, Ar *m*-NO_2), 7.50 (s, 1H, N$\underline{H}$), 7.45 (s, 3H, triazole), 7.27–7.14 (m, 45H, Ar), 4.46–4.24 (m, 30H, O-$\underline{CH_2}$-Ph, H-8, H-9), 3.84 (m, 9H, H-10, H-4), 3.71 (d, *J* = 3.9 Hz, 3H, H-3), 3.38 (m, 6H, H-6), 3.24 (m, 3H, Ha-7), 3.09 (d, *J* = 10.2 Hz, 3H, Ha-5), 2.77 (m, 6H, Hb-7, H-2), 2.60 (dd, *J* = 10.2, 5.1 Hz, 3H, Hb-5). **^{13}C NMR** (50 MHz, $CDCl_3$) δ ppm = 165.4 (s, 1C, C═O), 149.3 (s, 1C, $\underline{C}$-NO_2), 144.3 (s, 3C, triazole), 140.6 (s, 1C, Ar *o*-NO_2), 138.0–137.9 (s, 9C, Ar), 128.6–127.7 (d, 47C, Ar, Ar *m*-NO_2), 123.5 (d, 2C, Ar *o*-NO_2), 123.3 (t, 3C, triazole), 84.9 (d, 3C, C-3), 81.4 (d, 3C, C-4), 73.2, 71.5, 71.2 (t, 9C, O-$\underline{CH_2}$-Ph), 71.1 (t, 3C, C-6), 69.0, 68.7 (6C, C-2, C-10), 64.5 (t, 3C, C-9), 60.6 (s, 1C, *scaffold*), 57.3 (t, 3C, C-5), 54.3 (t, 3C, C-7), 48.9 (t, 3C, C-9). **IR** ($CDCl_3$) ν = 3415, 3088, 3066, 3032, 2925, 2863, 1724, 1667, 1603, 1526, 1496, 1454, 1347, 1279, 1054 cm^{-1}. **MS-ESI** (*m/z*, %) = 1823.6 (MNa^+, 97).

Synthesis of deprotected trivalent iminosugar bearing the 4-nitrobenzene moiety 39: A solution of compound **38** (38 mg, 0.021 mmol) in dry CH_2Cl_2 (2.1 mL) was cooled to 0 °C (ice bath) under nitrogen atmosphere and a 1 M solution of BCl_3 in hexane (0.57 mL) was added. The reaction mixture was left to reach room temperature and stirred for 15 h, when a TLC analysis (eluent AcOEt) attested the disappearance of the starting material **38** (R_f = 0.45). EtOH was added until a homogeneous mixture was obtained, then the solvents were evaporated under a vacuum. The resulting crude was purified via FCC (CH_2Cl_2/MeOH/ 6% NH_4OH 6: 2:0.5) affording pure **39** (20 mg, 0.020 mmol) with a 95% yield. $[\alpha]_D^{25}$ = −3.4 (c = 0.705, CH_3OH). **^{1}H NMR** (400 MHz, CD_3OD) δ ppm = 8.29 (m, 2H, Ar *o*-NO_2), 8.13 (s, 3H, triazole), 7.95 (m, 2H, Ar *m*-NO_2), 4.75 (m, 6H, H-8), 4.60 (s, 6H, H-9), 4.10 (m, 3H, H-4), 3.91 (m, 3H, H-3), 3.85 (s, 6H, H-10), 3.74 (m, 9H, H-6, Ha-7), 3.31 (m, 6H, Hb-7, Ha-5), 3.13 (m, 6H Hb-5, H-2). **^{13}C NMR** (50 MHz, CD_3OD) δ ppm = 167.2 (s, 1C, C═O), 149.5 (s, 1C, $\underline{C}$-

NO_2), 144.6 (s, 3C, triazole), 142.5 (s, 1C, Ar *p*-NO_2), 128.5 (d, 2C, Ar *m*-NO_2), 124.7 (d, 2C, Ar *o*-NO_2), 123.2 (d, 3C, triazole), 77.3 (d, 3C, C-3), 76.0 (d, 3C, C-4), 75.0 (d, 3C, C-2), 67.8 (t, 3C, C-10), 63.7 (t, 3C, C-9), 60.8 (s, 1C, *scaffold*), 60.0 (t, 3C, C-6), 59.6 (t, 3C, C-5), 55.0 (t, 3C, C-7), 44.2 (t, 3C, C-8). **MS-ESI** (*m/z*, %) = 1013.34 (MNa^+, 100).

Synthesis of 4-nitro-*N*-propylbenzamide (40): To a solution of 4-nitrobenzoyl chloride (52 mg, 0.28 mmol) in dry pyridine, under nitrogen atmosphere, propan-1-amine (35 µL, 0.42 mmol) was added. The reaction mixture was stirred at room temperature for 18 h, when a TLC analysis (eluent PE/AcOEt 10:1) attested the disappearance of 4-nitrobenzoyl chloride (R_f = 0.58) and the formation of a new product (R_f = 0.78). The pyridine was evaporated under a vacuum and the resulting crude was purified by FCC (PE/AcOEt 3:2), leading to compound **40** (44 mg, 0.021 mmol) with a 76% yield. **^{1}H NMR** (400 MHz, CD_3Cl_3) [53] δ ppm =: 8.22 (d, *J* = 8.8 Hz, 2H, Ar *o*-NO_2), 7.91 (d, *J* = 8.8 Hz, 2H, Ar *m*-NO_2), 6.56 (br s, 1H, NH), 3.41 (dd, *J* = 7.3, 6.9 Hz, 2H), 1.63 (sest, *J* = 7.4 Hz, 2H), 0.96 (t, *J* = 7.4 Hz, 3H).

Synthesis of 4-nitro-*N*-(3-pyrrolidin-1yl-propyl)benzamide (41): To a solution of *N*-(3-bromopropyl)-4-nitrobenzamide [66] (15 mg, 0.052 mmol) in CH_3CN (1 mL), pyrrolidine (0.77 µL, 0.936 mmol) was added and the reaction mixture was stirred at reflux for 18 h, until a \TLC analysis (eluent Hexane/AcOEt 1:1) attested the disappearance of *N*-(3-bromopropyl)-4-nitrobenzamide (R_f = 0.57). The mixture was concentrated under a vacuum and the resulting crude was purified via FCC (Hexane/AcOEt 1:3), affording pure **41** (13.0 mg, 0.047 mmol) with a 90% yield. **^{1}H NMR** (400 MHz, $CDCl_3$) δ ppm = 9.01 (br s, 1H, O = CN*H*), 8.26 (d, *J* = 8.6 Hz, 2H, Ar), 8.15 (d, *J* = 8.6 Hz, 2H, Ar), 3.65 (dd, *J* = 10.8, 5.2 Hz, 2H, $\underline{CH_2}$NHC = O), 3.10–3.05 (m, 6H), 2.13–2.02 (m, 6H). **^{13}C NMR** (100 MHz, $CDCl_3$) δ ppm = 165.3 (s, 1C, C=O), 149.6 (s, 1C, $\underline{C}$-NO_2), 139.4 (s, 1C, Ar *p*-NO_2), 128.5 (d, 2C, Ar *m*-NO_2), 123.6 (d, 2C, Ar *o*-NO_2), 53.7, 53.4 (t, 3C), 37.8 (t, 1C,CH_2NHC = O), 25.0, 23.3 (t, 3C). **MS-ESI** (*m/z*, %) = 278.21 (MH^+, 100).

4.2. Biology

4.2.1. Expression and purification of recombinant human PTP-1B

The PTP-1B enzyme was purified as a fusion protein from TB1 bacterial cell lines. pGEX-2 T expression vectors containing the full sequence of PTP-1B cloned downstream of the GST sequence were used to transform the TB1 E. coli strain. The recombinant fusion protein was purified from bacterial lysate using single step affinity chromatography with a glutathione-agarose resin. Fractions containing the fusion protein were collected and concentrated up to a volume of 5 mL. The cleavage of the fusion protein was carried out by incubating the solution with 1.25 U of human thrombin for 3 h at 37 °C. Then the active phosphatase was purified from GST and thrombin by gel filtration on a Superdex G75 column. The enzyme purity was determined by SDS-PAGE.

4.2.2. Enzymatic assays with PTP1B

The assays were carried out at 37 °C using aliquots of purified recombinant human PTP1B and *p*-nitrophenylphosphate (pNPP) as a synthetic substrate (2.5 mM, a value corresponding to the K_m of the enzyme). All assays were carried out in 0.075 M of β,β-dimethyl glutarate pH 7.0 buffer, containing 1 mM EDTA and 1 mM dithiothreitol. The final volume of each test was 1 mL. Assay solutions were incubated at 37 °C for 10 min. Then, the reactions were started by adding aliquots of the enzyme. The reactions were stopped by adding 4 mL of 0.1 M KOH after 30 min. The released p-nitrophenolate ion was determined by reading the absorbance at 400 nm (ε = 18,000 M^{-1} cm^{-1}).

The IC_{50} values were determined by measuring the residual enzyme activity in the presence of increasing inhibitor concentration and a fixed substrate concentration corresponding to that of Km of the enzyme. Fifteen different inhibitor concentrations were used for every compound. Data obtained were normalized with respect to the control sample and fitted using the following equation:

$$\frac{\grave{Vi}}{V0} = \frac{Max-Min}{1 + (\frac{X}{IC50})^{slope}} + Min$$

where Vi/V0, represents the ratio between the activity measured in the presence of the inhibitor (Vi) and the activity of the enzyme measured in the absence of inhibitor (V0), while the parameter "x" represents the concentration of inhibitor. All assays were carried out in triplicate.

The action mechanism of compounds was determined by analysing the dependence of main kinetic parameters, Km and Vmax, from the inhibitor concentrations. The kinetic parameters, Km and Vmax, were determined measuring the initial hydrolysis rates in the presence of increasing substrate concentrations. Data obtained were fitted using the Michaelis-Menten equation. Inhibition constant (Ki) were determined using the following equation:

$$1/Vmax_{app} = 1/(Vmax * Ki)[I] + 1/Vmax \quad (1)$$

4.2.3. Enzymatic assays with porcine pancreatic α-glucosidase

The ability of compounds to inhibit α-glucosidase was assayed by using a spectrophotometric method. We prepared vials containing 300 µL of reaction mixture. Each vial contained 170 µL of 100 mM phosphate buffer (pH 6.8), 100 µL of 2.5 mM pNPG, and 10 µL of the compounds dissolved in DMSO. The final concentration of compounds in each vial was 0.66 mM. Samples were incubated for 10 min at 37 °C and then diluted with 20 µL of α-glucosidase [2 U/mL in 10 mM phosphate buffer (pH 6.8)]. The vials were incubated at 37 °C for a further 30 min. The reactions were stopped by the addition of 700 µL of 0.2 M sodium carbonate solution. The absorbance of samples was recorded at 405 nm using an Ultrospec 2000 UV/visible spectrophotometer (Pharmacia Biotech). The control test was carried out using the same reaction mixture containing 10 µL of DMSO, the solvent used for dilute compounds.

4.2.4. Enzymatic assays with α-glucosidase from Saccharomyces cerevisiae and towards amyloglucosidase from Aspergillus niger

The % of inhibition towards the corresponding glycosidase was determined in the presence of 1 mM of the inhibitor on the well. Each enzymatic assay (final volume 0.12 mL) contains 0.01 to 0.5 units/mL of the enzyme and 10 mM aqueous solution of the *p*-nitrophenyl α-glucopyranoside (substrate) buffered to the optimal pH of the enzyme (pH = 7.0 for α-glucosidase from *Saccharomyces cerevisiae* and pH = 5.0 for amyloglucosidase from *Aspergillus niger*). Enzyme and inhibitor were preincubated for 5 min at rt, and the reaction started by the addition of the substrate. After 20 min of incubation at 37 °C, the reaction was stopped by the addition of 0.1 mL of sodium borate solution (pH 9.8). The *p*-nitrophenolate formed was measured by visible absorption spectroscopy at 405 nm. Under these conditions, the *p*-nitrophenolate released led to optical densities linear with both reaction time and concentration of the enzyme; thus, the measured absorbance can be transformed into % of inhibition. The IC_{50} value (concentration of inhibitor required for 50% inhibition of enzyme activity) was determined from plots of % inhibition *versus* inhibitor concentration (eight different concentrations were used). For the IC_{50} plot, each percentage of inhibition was obtained in duplicate and the average value was given (see IC_{50} graphs in Supplementary data).

4.2.5. Inhibition assay towards lysosomal enzyme acid α-glucosidase (EC 3.2.1.20) [59,60]

Our laboratories' whole collection of iminosugars was tested towards α-glucosidase from lymphocytes isolated from healthy donors' flesh blood (controls), using the protocol with Lymphoprep™ [67]. Isolated lymphocytes were disrupted by sonication and the micro BCA protein assay kit (Sigma-Aldrich) was used to set up the protein amount for the enzymatic assay, according to the manufacturer's instructions.

α-Glucosidase activity was measured in a flat–bottomed 96 well plate: iminosugar solution (3 μL), 4.29 μg/μL lymphocytes homogenate (7 μL) and 20 μL of substrate solution of 4-methylumbelliferyl-α-D-glucopyranoside (Sigma-Aldrich) in Na acetate buffer (0.2 M, pH 4.0) were incubated for 1 h at 37 °C. The reaction was stopped by the addition of a solution of sodium carbonate (0.5 M, 0.0025% triton X100, pH 10.7, 200 μL) and fluorescence was measured in a SpectraMax M2 microplate reader (Molecular-Devices) using an excitation wavelength of 365 nm and an emission wavelength of 435 nm. Percentages of α-glucosidase inhibition were given with respect to the control (without iminosugar). Experiments were performed in triplicate.

The IC_{50} values against the human acid α-glucosidase inhibitors were determined by measuring the initial hydrolysis rate under fixed 4-methylumbelliferyl-α-D-glucoside concentration (1.47 mM). Data were obtained using the previously reported method (see the Supporting Information file for further details and graphs) [68].

4.2.6. Inhibition assay towards lysosomal enzyme acid β-glucosidase (also known as glucocerebrosidase, GCase; EC 3.2.1.45) [69–71]

Our laboratories' whole collection of iminosugars was tested towards GCase from leukocytes isolated from healthy donors (controls). Isolated leukocytes were disrupted by sonication and the micro BCA protein assay kit (Sigma-Aldrich) was used to set up the protein amount for the enzymatic assay, according to the manufacturer instructions. GCase activity was measured in a flat–bottomed 96 well plate: iminosugar solution (3 μL), 4.29 μg/μL leukocytes homogenate (7 μL) and 20 μL of substrate solution of 4-methylumbelliferyl-β-D-glucoside (Sigma-Aldrich) in citrate/phosphate buffer (0.1 M/0.2 M, pH 5.8) containing 0.3% sodium taurocholate and 0.15% triton X100 were incubated for 1 h at 37 °C. The reaction was stopped by the addition of a solution of sodium carbonate (0.5 M, 0.0025% triton X100, pH 10.7, 200 μL) and fluorescence was measured in a SpectraMax M2 microplate reader (Molecular-Devices) using an excitation wavelength of 365 nm and an emission wavelength of 435 nm. Percentages of GCase inhibition were given with respect to the control (without iminosugar). Experiments were performed in triplicate.

4.2.7. Ex vivo assay

Ex vivo tests were carried out using human liver cell lines (HepG2 cells obtained from the American Type Culture Collection (ATCC)). Cells were grown in complete medium (DMEM) containing 10% fetal bovine serum until about 70% confluence. Then, cells were starved for 20 h before stimulation with 10 nM insulin or incubation with compounds.

Negative controls were obtained by incubating samples with DMSO, the solvent used to dilute each inhibitor. After an appropriate time, samples were lysed using 1x LAEMMLI sample buffer. Protein extracts were separated by SDS-PAGE, transferred to PVDF membrane by western blot. Detection of activated forms of Akt kinase was carried out using specific antibodies and Phospho-Akt (Ser473) antibody (Santa Cruz Biotechnology).

Declaration of interest

None.

Acknowledgements

We thank MIUR-Italy ("Progetto Dipartimenti di Eccellenza 2018-2022" allocated to Department of Chemistry "Ugo Schiff"). Ministerio de Economía y Competitividad of Spain (CTQ2016-77270-R) is also acknowledged for financial support. We also thank Fondazione CR Firenze for financial support and for a fellowship to CM (grant NO. 2016/0845), and the AMMeC and the Fondazione Ospedale Pediatrico A. Meyer ONLUS, Florence, Italy for continuing support. We also thank Prof. Andrea Trabocchi for helpful discussions. Finally, we thank University of Florence – Italy for financial support (Fondi di Ateneo, ex-60%). We also thank Dr. Alessandro Pratesi for technical assistance.

Appendix A. Supplementary material

Supplementary data contains ^{1}H and ^{13}C NMR spectra of all new compounds, kinetic analysis toward PTP1B of compounds **9** and **13**, evaluation of the inhibitory power of compound **40** and **41** on PTP1B, and IC_{50} graphs towards glucosidases. Supplementary data to this article can be found online at https://doi.org/10.1016/j.bioorg.2019.03.053.

References

[1] K. Ogurtsova, J.D. da Rocha Fernandes, Y. Huang, U. Linnenkamp, L. Guariguata, N.H. Cho, D. Cavan, J.E. Shaw, L.E. Makaroff, IDF diabetes Atlas: global estimates for the prevalence of diabetes for 2015 and 2040, Diabetes Res. Clin. Pract. 128 (2017) 40–50, https://doi.org/10.1016/j.diabres.2017.03.024.
[2] H.J. Dean, E.A.C. Sellers, Children have type 2 diabetes too: an historical perspective, Biochem. Cell Biol. 93 (2015) 425–429, https://doi.org/10.1139/bcb-2014-0152.
[3] J.D. Hughes, Y. Wibowo, B. Sunderland, K. Hoti, The role of the pharmacist in the management of type 2 diabetes: current insights and future directions, Integr. Pharm. Res. Pract 6 (2017) 15–27, https://doi.org/10.2147/IPRP.S103783.
[4] R.J. Heine, M. Diamant, J.-C. Mbanya, D.M. Nathan, Management of hyperglycaemia in type 2 diabetes: the end of recurrent failure? BMJ 333 (7580) (2006) 1200–1204, https://doi.org/10.1136/bmj.39022.462546.80.
[5] M. Elchebly, P. Payette, E. Michaliszyn, W. Cromlish, S. Collins, A.L. Loy, D. Normandin, A. Cheng, J. Himms-Hagen, C.-C. Chan, C. Ramachandran, M.J. Gresser, M.L. Tremblay, B.P. Kennedy, Increased insulin sensitivity and obesity resistance in mice lacking the protein tyrosine phosphatase-1B gene, Science 283 (1999) 1544–1548, https://doi.org/10.1126/science.283.5407.1544.
[6] M.Y. Ali, D.H. Kim, S.H. Seong, H.-R. Kim, H.A. Jung, J.S. Choi, α-Glucosidase and protein tyrosine phosphatase 1B inhibitory activity of plastoquinones from marine brown alga *Sargassum serratifolium*, Mar. Drugs 15 (2017) E368, https://doi.org/10.3390/md15120368.
[7] S.H. Seong, A. Roy, H.A. Jung, H.J. Jung, J.S. Choi, Protein tyrosine phosphatase 1B and α-glucosidase inhibitory activities of *Pueraria lobata* root and its constituents, J. Ethnopharmacol. 194 (2016) 706–716, https://doi.org/10.1016/j.jep.2016.10.007.
[8] M.Y. Ali, S. Jannat, H.A. Jung, H.O. Jeong, H.Y. Chung, J.S. Choi, Coumarins from *Angelica decursiva* inhibit α-glucosidase activity and protein tyrosine phosphatase 1B, Chem.-Biol. Interact. 252 (2016) 93–101, https://doi.org/10.1016/j.cbi.2016.04.020.
[9] H.A. Jung, M.Y. Ali, J.S. Choi, Promising inhibitory effects of anthraquinones, naphthopyrone, and naphthalene glycosides, from *Cassia obtusifolia* on α-glucosidase and human protein tyrosine phosphatases 1B, Molecules 22 (2017) E28, https://doi.org/10.3390/molecules22010028.
[10] S.G. Wubshet, Y.T. Tahtah, A.M. Heskes, K.T. Kongstad, I. Pateraki, B. Hamberger, B.L. Möller, D. Staerk, Identification of PTP1B and α-glucosidase inhibitory serrulatanes from *Eremophila* spp. by combined use of dual high-resolution PTP1B and α-glucosidase inhibition profiling and HPLC-HRMS-SPE-NMR, J. Nat. Prod. 79 (2016) 1063–1072, https://doi.org/10.1021/acs.jnatprod.5b01128.
[11] Y.H. Song, Z. Uddin, Y.M. Jin, Z. Li, M.J. Curtis-Long, K.D. Kim, J.K. Cho, K.H. Park, Inhibition of protein tyrosine phosphatase (PTP1B) and α-glucosidase by geranylated flavonoids from *Paulownia tomentosa*, J. Enz. Inhib. Med. Chem. 32 (2017) 1195–1202, https://doi.org/10.1080/14756366.2017.1368502.
[12] M.T. Ha, S.H. Seong, T.D. Nguyen, W.-K. Cho, K.J. Ah, J.Y. Ma, M.H. Woo, J.S. Choi, B.S. Min, Chalcone derivatives from the root bark of *Morus alba* L. act as inhibitors of PTP1B and α-glucosidase, Phytochemistry 155 (2018) 114–125, https://doi.org/10.1016/j.phytochem.2018.08.001.
[13] E. Beutler, G.A. Grabowski, Gaucher disease, in: C.R. Scriver, A.L. Beaudet, W.S. Sly (Eds.), The Metabolic and Molecular Basis of Inherited Disease, McGraw-Hill, New York, 2001, pp. 3635–3668.
[14] M. Langeveld, K.J.M. Ghauharali, H.P. Sauerwein, M.T. Ackermans, J.E.M. Groener, C.E.M. Hollak, J.M.F.G. Aerts, M.J. Serlie, Type 1 Gaucher disease, a glycosphingolipid storage disorder, is associated with insulin resistance, J. Clin. Endocrinol. Metab. 93 (2008) 845–851, https://doi.org/10.1210/jc.2007-1702.
[15] M. Langeveld, M. de Fost, J.M.F.G. Aerts, H.P. Sauerwein, C.E.M. Hollak, Overweight, insulin resistance and type II diabetes in type I Gaucher disease patients in relation to enzyme replacement therapy, Blood Cells Mol. Dis. 40 (2008) 428–432, https://doi.org/10.1016/j.bcmd.2007.09.002.
[16] S.K. Ucar, M. Coker, M. Argin, S. Akman, S. Kara, D.G. Simsek, S. Darcan, A crosssectional, mono-centric pilot study of insulin resistance in enzyme replacement therapy patients with Gaucher type 1 without overweight, Mol. Genet. Metab. 96 (2009) 50–51, https://doi.org/10.1016/j.ymgme.2008.10.001.
[17] F. Nascimbeni, A. Dalla Salda, F. Carubbi, Energy balance, glucose and lipid metabolism, cardiovascular risk and liver disease burden in adult patients with type 1 Gaucher disease, Blood Cells Mol. Dis. 68 (2018) 74–80, https://doi.org/10.1016/j.bcmd.2016.10.012.
[18] M. Fuller, Sphingolipids: the nexus between Gaucher disease and insulin resistance, Lip. Health Dis. 9 (2010) 113, https://doi.org/10.1186/1476-511X-9-113.

[19] R.E. Boyd, G. Lee, P. Rybczynski, E.R. Benjamin, R. Khanna, B.A. Wustman, K.J. Valenzano, Pharmacological chaperones as therapeutics for lysosomal storage diseases, J. Med. Chem. 56 (2013) 2705–2725, https://doi.org/10.1021/jm301557k.

[20] E.M. Sánchez-Fernández, J.M. García Fernández, C. Ortiz Mellet, Glycomimetic-based pharmacological chaperones for lysosomal storage disorders: lessons from Gaucher, GM1-gangliosidosis and Fabry diseases, Chem. Commun. 52 (2016) 5497–5515, https://doi.org/10.1039/C6CC01564F.

[21] G. Navarrete-Vazquez, P. Paoli, I. Leon-Rivera, R. Villalobos-Molina, J.L. Medina-Franco, R. Ortiz-Andrade, S. Estrata-Soto, G. Camici, D. Diaz-Coutiño, I. Gallardo-Ortiz, K. Martinez-Mayorga, H. Moreno-Díaz, Synthesis, in vitro and computational studies of protein tyrosine phosphatase 1B inhibition of a small library of 2-arylsulfonylaminobenzothiazoles with antihyperglycemic activity, Bioorg. Med. Chem. 17 (2009) 3332–3341, https://doi.org/10.1016/j.bmc.2009.03.042.

[22] K. Varshney, S. Gupta, N. Rahuja, A.K. Rawat, N. Singh, A.K. Tamarkar, A.K. Srivastava, A.K. Saxena, Synthesis, structure-activity relationship and docking studies of substituted aryl thiazolyl phenylsulfonamides as potential protein tyrosine phosphatase 1B inhibitors, ChemMedChem 7 (2012) 1185–1190, https://doi.org/10.1002/cmdc.201200197.

[23] P. Compain, O.R. Martin (Eds.), Iminosugars: from Synthesis to Therapeutic Applications, Wiley VCH, New York, 2007.

[24] K. Yasuda, H. Kizu, T. Yamashita, Y. Kameda, A. Kato, R.J. Nash, G.W.J. Fleet, R.J. Molyneux, N. Asano, New sugar-mimic alkaloids from the pods of *Angylocalyx pynaertii*, J. Nat. Prod. 65 (2002) 198–202, https://doi.org/10.1021/np010360f.

[25] J.M.F.G. Aerts, R. Ottenhoff, A.S. Powlson, A. Grefhorst, M. van Eijk, P.F. Dubbelhuis, J. Aten, F. Kuipers, M.J. Serlie, T. Wennekes, J.K. Sethi, S. O'Rahilly, H.S. Overkleeft, Pharmacological inhibition of glucosylceramide synthase enhances insulin sensitivity, Diabetes 56 (2007) 1341–1349, https://doi.org/10.2337/db06-1619.

[26] F. Cardona, C. Parmeggiani, E. Faggi, C. Bonaccini, P. Gratteri, L. Sim, T.M. Gloster, S. Roberts, G.J. Davies, D.R. Rose, A. Goti, Total syntheses of Casuarine and its 6-*O*-α-Glucoside: complementary inhibition towards glycoside hydrolases of the GH31 and GH37 families, Chem. Eur. J. 15 (2009) 1627–1636, https://doi.org/10.1002/chem.200801578.

[27] L.J. Scott, C.M. Spencer, Miglitol: a review of its therapeutic potential in type 2 diabetes mellitus, Drugs 59 (2000) 521–549, https://doi.org/10.2165/00003495-200059030-00012.

[28] C. Parmeggiani, S. Catarzi, C. Matassini, G. D'Adamio, A. Morrone, A. Goti, P. Paoli, F. Cardona, Human acid β-glucosidase inhibition by carbohydrate derived iminosugars: towards new pharmacological chaperones for Gaucher disease, ChemBioChem 16 (2015) 2054–2064, https://doi.org/10.1002/cbic.201500292.

[29] G. D'Adamio, C. Matassini, C. Parmeggiani, S. Catarzi, A. Morrone, A. Goti, P. Paoli, F. Cardona, Evidence for a multivalent effect in inhibition of sulfatases involved in lysosomal storage disorders (LSDs), RSC Adv. 6 (2016) 64847–64851, https://doi.org/10.1039/C6RA15806D.

[30] F. Cardona, A. Goti, S. Picasso, P. Vogel, A. Brandi, Polyhydroxypyrrolidine glycosidase inhibitors related to (+)-lentiginosine, J. Carbohydr. Chem. 19 (2000) 585–601, https://doi.org/10.1080/07328300008544101.

[31] A. Goti, F. Cardona, A. Brandi, S. Picasso, P. Vogel, (1*S*,2*S*,7*R*,8a*S*)- and (1*S*,2*S*,7*S*,8a*S*)-Trihydroxyoctahydroindolizine: two new glycosidase inhibitors by nitrone cycloaddition strategy, Tetrahedron: asymmetry 7 (1996) 1659–1674, https://doi.org/10.1016/0957-4166(96)00200-5.

[32] C. Matassini, S. Mirabella, A. Goti, F. Cardona, Double reductive amination and selective Strecker reaction of a d-Lyxaric aldehyde: synthesis of diversely functionalized 3,4,5-trihydroxypiperidines, Eur. J. Org. Chem. (2012) 3920–3924, https://doi.org/10.1002/ejoc.201200587.

[33] C. Matassini, S. Mirabella, X. Ferhati, C. Faggi, I. Robina, A. Goti, E. Moreno-Clavijo, A.J. Moreno-Vargas, F. Cardona, Polyhydroxyamino-piperidine-type iminosugars and pipecolic acid analogues from a d-mannose-derived aldehyde, Eur. J. Org. Chem. (2014) 5419–5432, https://doi.org/10.1002/ejoc.201402427.

[34] C. Bonaccini, M. Chioccioli, C. Parmeggiani, F. Cardona, Re D. Lo, G. Soldaini, P. Vogel, C. Bello, A. Goti, P. Gratteri, Synthesis biological evaluation and docking studies of casuarine analogs: effects of structural modifications at ring B on inhibitory activity towards glucoamylase, Eur. J. Org. Chem. (2010) 5574–5585, https://doi.org/10.1002/ejoc.201000632.

[35] F. Cardona, A. Goti, C. Parmeggiani, P. Parenti, M. Forcella, P. Fusi, L. Cipolla, S.M. Roberts, G.J. Davies, T.M. Gloster, Casuarine-6-*O*-α-d-glucoside and its analogues are tight binding inhibitors of insect and bacterial trehalases, Chem. Commun. 46 (2010) 2629–2631, https://doi.org/10.1039/B926600C.

[36] G. D'Adamio, A. Goti, C. Parmeggiani, E. Moreno-Clavijo, I. Robina, F. Cardona, Total synthesis of (+)-hyacinthacine A_1, (+)-7a-*epi*-hyacinthacine A_1, 6(*R*)–6-hydroxyhyacinthacine A_1 and 6(*S*)-6-hydroxy-7a-*epi*-hyacinthacine A_1, Eur. J. Org. Chem. (2011) 7155–7162, https://doi.org/10.1002/ejoc.201101096.

[37] G. D'Adamio, C. Parmeggiani, A. Goti, A.J. Moreno-Vargas, E. Moreno-Clavijo, I. Robina, F. Cardona, 6-Azido hyacinthacine A_2 gives a straightforward access to the first multivalent pyrrolizidine architectures, Org. Biomol. Chem. 12 (2014) 6250–6266, https://doi.org/10.1039/c4ob01117a.

[38] G. D'Adamio, A. Sgambato, M. Forcella, S. Caccia, C. Parmeggiani, M. Casartelli, P. Parenti, D. Bini, L. Cipolla, P. Fusi, F. Cardona, New synthesis and biological evaluation of uniflorine A derivatives: towards specific insect trehalase inhibitors, Org. Biomol. Chem. 13 (2015) 886–892, https://doi.org/10.1039/C4OB02016B.

[39] D. Martella, F. Cardona, C. Parmeggiani, F. Franco, J.A. Tamayo, I. Robina, E. Moreno-Clavijo, A.J. Moreno-Vargas, A. Goti, Synthesis and glycosidase inhibition studies of 5-methyl-Substituted tetrahydroxyindolizidines and -pyrrolizidines related to natural hyacinthacines B, Eur. J. Org. Chem. (2013) 4047–4056, https://doi.org/10.1002/ejoc.201300103.

[40] D. Martella, G. D'Adamio, C. Parmeggiani, F. Cardona, E. Moreno-Clavijo, I. Robina, A. Goti, Cycloadditions of sugar-derived nitrone targeting polyhydroxylated indolizidines, Eur. J. Org. Chem. (2016) 1588–1598, https://doi.org/10.1002/ejoc.201501427.

[41] H.D. Agnew, R.D. Rohde, S.W. Millward, A. Nag, W.-S. Yeo, J.E. Hein, S.M. Pitram, A.A. Tariq, V.M. Burns, R.J. Krom, V.V. Fokin, K.B. Sharpless, J.R. Heath, Iterative in situ click chemistry creates antibody-like protein-capture agents, Angew. Chem. Int. Ed. 48 (27) (2009) 4944–4948, https://doi.org/10.1002/anie.v48:2710.1002/anie.200900488.

[42] M. Meldal, C.W. Tornøe, Cu-catalyzed azide – alkyne cycloaddition, Chem. Rev. 108 (2008) 2952–3015, https://doi.org/10.1021/cr0783479.

[43] S. Desvergnes, Y. Valleè, S. Py, Novel polyhydroxylated cyclic nitrones and *N*-Hydroxypyrrolidines through BCl_3-mediated deprotection, Org. Lett. 10 (2008) 2967–2970, https://doi.org/10.1021/ol8007759.

[44] S.-K. Choi (Ed.), Synthetic Multivalent Molecules: Concepts and Biomedical Applications, Wiley, New Jersey, 2004.

[45] L.L. Kiessling, J.E. Gestwicki, L.E. Strong, Synthetic multivalent ligands as probes of signal transduction, Angew. Chem. Int. Ed. 45 (15) (2006) 2348–2368, https://doi.org/10.1002/anie.200502794.

[46] A. Imberty, Y.M. Chabre, R. Roy, Glycomimetics and glycodendrimers as high affinity microbial anti-adhesins, Chem. Eur. J. 14 (25) (2008) 7490–7499, https://doi.org/10.1002/chem.200800700.

[47] D. Deniaud, K. Julienne, S.G. Gouin, Insights in the rational design of synthetic multivalent glycoconjugates as lectin ligands, Org. Biomol. Chem. 9 (2011) 966–979, https://doi.org/10.1039/C0OB00389A.

[48] Á. Martinez, C. Ortiz Mellet, J.M. García Fernández, Cyclodextrin-based multivalent glycodisplays: covalent and supramolecular conjugates to assess carbohydrate–protein interactions, Chem. Soc. Rev. 42 (2013) 4746–4773, https://doi.org/10.1039/C2CS35424A.

[49] S.G. Gouin, Multivalent inhibitors for carbohydrate-processing enzymes: beyond the "Lock-and-Key" concept, Chem. Eur. J. 20 (2014) 11616–11628, https://doi.org/10.1002/chem.201402537.

[50] P. Compain, A. Bodlenner, The multivalent effect in glycosidase inhibition: a new, rapidly emerging topic in glycoscience, ChemBioChem 15 (2014) 1239–1251, https://doi.org/10.1002/cbic.201402026.

[51] R. Zelli, J.-F. Longevial, P. Dumy, A. Marra, Synthesis and biological properties of multivalent iminosugars, New J. Chem. 39 (2015) 5050–5074, https://doi.org/10.1039/C5NJ00462D.

[52] N. Kanfar, E. Bartolami, R. Zelli, A. Marra, J.-Y. Winum, S. Ulrich, P. Dumy, Emerging trends in enzyme inhibition by multivalent nanoconstructs, Org. Biomol. Chem. 13 (2015) 9894–9906, https://doi.org/10.1039/C5OB01405K.

[53] C. Matassini, C. Parmeggiani, F. Cardona, A. Goti, Are enzymes sensitive to the multivalent effect? Emerging evidence with glycosidases, Tetrahedron Lett. 57 (49) (2016) 5407–5415, https://doi.org/10.1016/j.tetlet.2016.10.080.

[54] Y.M. Chabre, C. Contino-Pépin, V. Placide, T.C. Shiao, R. Roy, Expeditive synthesis of glycodendrimer scaffolds based on versatile TRIS and mannoside derivatives, J. Org. Chem. 73 (2008) 5602–5605, https://doi.org/10.1021/jo8008935.

[55] V.D. Bock, D. Speijer, H. Hiemstra, J.H. van Maarseveen, 1,2,3-Triazoles as peptide bond isosteres: synthesis and biological evaluation of cyclotetrapeptide mimics, Org. Biomol. Chem. 5 (2007) 971–975, https://doi.org/10.1039/B616751A.

[56] J. Hou, X. Liu, J. Shen, G. Zhao, P.G. Wang, The impact of click chemistry in medicinal chemistry, Expert Opin. Drug Discov. 7 (2012) 489–501, https://doi.org/10.1517/17460441.2012.682725.

[57] H. Yang, W. Hu, S. Deng, T. Wu, H. Cen, Y. Chen, D. Zhang, B. Wang, Catalyst-free amidation of aldehyde with amine under mild conditions, New J. Chem. 39 (8) (2015) 5912–5915, https://doi.org/10.1039/C5NJ01372K.

[58] G. Derosa, P. Maffioli, α-Glucosidase inhibitors and their use in clinical practice, Arch. Med. Sci. 8 (2012) 899–906, https://doi.org/10.5114/aoms.2012.31621.

[59] M.M.P. Hermans, M.A. Kroos, J. Van Beeumen, B.A. Oostra, A.J.J. Reuser, Human lysosomal α-glucosidase, J. Biol. Chem. 266 (1991) 13507–13512.

[60] M.M.P. Hermans, E. de Graaff, M.A. Kroos, H.A. Wisselaar, B.A. Oostra, A.J.J. Reuser, Identification of a point mutation in the human lysosomal α-glucosidase gene causing infantile glycogenosis type II, Biochem. Biophys. Res. Commun. 179 (2) (1991) 919–926, https://doi.org/10.1016/0006-291X(91)91906-S.

[61] F.M. Platt, A. D'Azzo, B.L. Davidson, E.F. Neufeld, C.J. Tifft, Lysosomal storage diseases, Nat Rev Dis Primers 4 (1) (2018), https://doi.org/10.1038/s41572-018-0025-4.

[62] S. Stratford, K.L. Hoehn, F. Liu, S.A. Summers, Regulation of insulin action by ceramide: dual mechanisms linking ceramide accumulation to the inhibition of Akt/protein kinase B, J. Biol. Chem. 279 (2004) 36608–36615, https://doi.org/10.1074/jbc.M406499200.

[63] X. Zhou, W.-J. Liu, J.-L. Ye, P.-Q. Huang, A versatile approach to pyrrolidine azasugars and homoazasugars based on a highly diastereoselective reductive benzyloxymethylation of protected tartarimide, Tetrahedron 63 (2007) 6346–6357, https://doi.org/10.1016/j.tet.2007.02.087.

[64] G. D'Adamio, M. Forcella, P. Fusi, P. Parenti, C. Matassini, X. Ferhati, C. Vanni, F. Cardona, Probing the influence of linker length and flexibility in the design and synthesis of new trehalase inhibitors, Molecules 23 (2018) 436, https://doi.org/10.3390/molecules23020436.

[65] W.-C. Cheng, C.-Y. Weng, W.-Y. Yun, S.-Y. Chang, Y.-C. Lin, F.-J. Tsai, F.-Y. Huang, Y.-R. Chen, Rapid modifications of *N*-substitution in iminosugars: Development of new β-glucocerebrosidase inhibitors and pharmacological chaperones for Gaucher disease, Bioorg. Med. Chem. 21 (2013) 5021–5028, https://doi.org/10.1016/j.bmc.2013.06.054.

[66] D.N. Reddy, E.N. Prabhakaran, Synthesis and isolation of 5,6-dihydro-4*H*-1,3-oxazine hydrobromides by autocyclization of *N*-(3-Bromopropyl)amides, J. Org.

Chem. 76 (2011) 680–683, https://doi.org/10.1021/jo101955q.
[67] C. Yeo, N. Saunders, D. Locca, A. Flett, M. Preston, P. Brookman, B. Davy, A. Mathur, S. Agrawal, Ficoll-Paque versus Lymphoprep: a comparative study of two density gradient media for therapeutic bone marrow mononuclear cell preparations, Regen. Med. 4 (2009) 689–696, https://doi.org/10.2217/rme.09.44.
[68] R. Ottanà, R. Maccari, J. Mortier, A. Caselli, S. Amuso, G. Camici, A. Rotondo, G. Wolber, P. Paoli, Synthesis, biological activity and structure-activity relationships of new benzoic acid-based protein tyrosine phosphatase inhibitors endowed with insulinomimetic effects in mouse C2C12 skeletal muscle cells, Eur. J. Med. Chem. 71 (2014) 112–127, https://doi.org/10.1016/j.ejmech.2013.11.001.
[69] L.B. Daniels, R.H. Glew, Beta-glucosidase assays in the diagnosis of Gaucher's disease, Clin. Chem. 28 (1982) 569–577.
[70] E. Beutler, W. Kuhl, F. Trinidad, R. Teplitz, H. Nadler, Beta-glucosidase activity in fibroblasts from homozygotes and heterozygotes for Gaucher's disease, Am. J. Hum. Genet. 23 (1971) 62–66.
[71] D.A. Wenger, C. Clark, M. Sattler, C. Wharton, Synthetic substrate beta-glucosidase activity in leukocytes: a reproducible method for the identification of patients and carriers of Gaucher's disease, Clin. Genet. 13 (1978) 145–153, https://doi.org/10.1111/j.1399-0004.1978.tb04242.x.